# Production of glucose dehydrogenase/cytochrome chimeras by sortagging and characterization of FAD binding constants in GMC-oxidoreductases

**Nikolić, Lorna**

**Master's thesis / Diplomski rad**

**2021**

*Degree Grantor / Ustanova koja je dodijelila akademski / stručni stupanj:* **University of Zagreb, Faculty of Food Technology and Biotechnology / Sveučilište u Zagrebu, Prehrambeno-biotehnološki fakultet**

*Permanent link / Trajna poveznica:* https://urn.nsk.hr/urn:nbn:hr:159:044091

UNIVERSITY OF ZAGREB
FACULTY OF FOOD TECHNOLOGY AND BIOTECHNOLOGY

# GRADUATE THESIS

Zagreb, September 2021

Lorna Nikolić
1164/BPI

# PRODUCTION OF GLUCOSE DEHYDROGENASE/CYTOCHROME CHIMERAS BY SORTAGGING AND CHARACTERIZATION OF FAD BINDING CONSTANTS IN GMC-OXIDOREDUCTASES

Experimental work for this Graduate thesis was done at the Department of Food Science and Technology, Biocatalyisis and Biosensing laboratory, BOKU – University of Natural Resources and Life Sciences, Vienna. The thesis was made under the guidance of associate professor Roland Ludwig, Ph.D., and with the help of postdoctoral researcher Erik Breslmayr, Ph.D., and Ph.D candidate Franziska Schachinger, MSc.

I would like to thank Associate professor Roland Ludwig, Ph.D. for giving me the opportunity to work on the experimental part of this thesis in his laboratoratory and with his team, my supervisors Erik Breslmayr, Ph.D. and Franziska Schachinger, MSc, my mentor Full professor Tonči Rezić, Ph.D. and my family and friends.
Thank you all for the patience, guidance and support provided.

**BASIC DOCUMENTATION CARD**

**Graduate Thesis**

**University of Zagreb**
**Faculty of Food Technology and Biotechnology**
**Department of Biochemical Engineering**
**Laboratory for Biochemical Engineering, Industrial Microbiology and Malting and Brewing Technology**

**Scientific area:** Biotechnical Sciences
**Scientific field:** Biotechnology

# PRODUCTION OF GLUCOSE DEHYDROGENASE/CYTOCHROME CHIMERAS BY SORTAGGING AND CHARACTERIZATION OF FAD BINDING CONSTANTS IN GMC-OXIDOREDUCTASES

*Lorna Nikolić. 1164/BPI*

**Abstract:** Majority of the growing market for biosensors is driven by medical diagnostics, especially glucose biosensors. Currently, the development of third generation mediatorless biosensors for glucose monitoring is underway. These biosensors employ GMC oxidoreductases as a biological recognition element and an electrochemical transducer for mediatorless detection and quantification of glucose. The problems of direct electron transfer (DET) to electrode, as well as low stability and substrate specificity still have to be overcome and were assesed in this thesis. In order to achieve DET, glucose dehydrogenase (GDH) and cytochrome *c* were postranslationally conjugated by sortase A to create a chimeric enzyme of improved perfomance mimicking DET capable cellobiose dehydrogenase (CDH). Furthermore, FAD binding constants of native *An*GOx, as well as recombinant *An*GOX, *Gc*GDH and *Mt*DH, expressed in *P. pastoris X33*, were determined by deflavination, followed by reflavination of apoenzymes with synthetic FAD. The goal was to create fusion protein capable of DET and to gain insights into the coffactor affinity.

**Keywords:** *glucose biosensors, GMC oxidoreductases, chimeric enzymes, dissociation constant, FAD*

**Thesis contains:** 64 pages, 26 figures, 18 tables, 36 references, 0 supplements

**Original in**: English

**Graduate Thesis in printed and electronic (**pdf format**) version is deposited in:** Library of the Faculty of Food Technology and Biotechnology**,** Kačićeva 23, Zagreb.

**Mentor:** *PhD. Tonči Rezić, Full professor*

**Principal mentor***:PhD. Roland Ludwig, Associate professor*

**Technical support and assistance**: *Erik Breslmayr, PhD. and Franziska Schachinger, MSc*

**Reviewers:**
1. PhD. *Blaženka Kos*, Full professor
2. PhD. *Roland Ludwig,* Associate professor
3. PhD. *Tonči Rezić,* Full professor
4. PhD. *Renata Teparić,* Full professor (substitute)

**Thesis defended:** 29. September 2021.

**TEMELJNA DOKUMENTACIJSKA KARTICA**

**Diplomski rad**

**Sveučilište u Zagrebu**
**Prehrambeno-biotehnološki fakultet**
**Zavod za biokemijsko inženjerstvo**
**Laboratorij za biokemijsko inženjerstvo, industrijsku mikrobiologiju i tehnologiju slada i piva**

**Znanstveno područje:** Biotehničke znanosti
**Znanstveno polje:** Biotehnologija

# PROIZVODNJA GLUKOZA DEHIDROGENAZA/CITOKROM KIMERNOG ENZIMA POMOĆU SORTAZE I KARAKTERIZACIJA KONSTANTI VEZANJA FAD-A KOD GMC-OKSIDOREDUKTAZA

*Lorna Nikolić, 1164/BPI*

**Sažetak:** Većinski udio u rastućem tržištu biosenzora zauzimaju potrebe medicinske dijagnostike za detekciju razine glukoze u krvi. Danas se aktivno radi na razvoju glukoznog biosenzora treće generacije, sastavni dio kojeg su GMC oksidoreduktaze, koje provode biokemijsku reakciju i pomoću elektrokemijskog transduktora (pretvarača signala), direktno i bez nusprodukata, prenose elektrone na elektrodu i omogućavaju detekciju i kvantifikaciju glukoze. Problemi koje je potrebno riješiti da bi ova tehnologija bila što pouzdanija su direktni elektronski transfer (DET) s enzima na elektrodu, te niska stabilnost i specifičnost enzima za supstrat. U svrhu postizanja DET-a proizveden je kimerni enzim koji oponaša elektronski transfer celobioza dehidrogenaze (CDH) povezivanjem glukoza dehidrogenaze (GDH) i citokroma *c* posttranslacijskom konjugacijom posredstvom sortaze A. Također, ispitane su i uspoređene konstante vezanja kofatora FAD-a GMC oksidoreduktaza od interesa (nativni *An*GOX, i rekombinantni *An*GOX, *Gc*GDH, *Mt*DH, proizvedeni pomoću *P. pastoris X33*) deflavinacijom i reflavinacijom pomoću sintetskog FAD-a. Cilj je bio proizvodnja sintetskog fuzijskog proteina s mogućnošću DET-a kako bi stekli uvid u afinitet kofaktora.

**Ključne riječi:** *glukozni biosenzori, GMC oksidoreduktaze, kimerni enzimi, konstanta disocijacije, FAD*

**Rad sadrži:** 64 stranice, 26 slika, 18 tablica, 36 literaturnih navoda, 0 priloga

**Jezik izvornika**: engleski

**Rad je u tiskanom i elektroničkom (pdf format) obliku pohranjen u:** Knjižnica Prehrambeno-biotehnološkog fakulteta, Kačićeva 23, Zagreb

**Mentor:** *prof.dr.sc. Tonči Rezić*

**Neposredni mentor:** *izv.prof.dr.sc. Roland Ludwig*

**Pomoć pri izradi**: *Erik Breslmayr, PhD i Franziska Schachinger, MSc*

**Stručno povjerenstvo za ocjenu i obranu:**
1. Prof.dr.sc. *Blaženka Kos*
2. Izv.prof.dr.sc. *Roland Ludwig*
3. Prof.dr.sc. *Tonči Rezić*
4. Prof.dr.sc. *Renata Teparić* (zamjena)

**Datum obrane:** 29. rujna 2021

# TABLE OF CONTENTS

# 1. INTRODUCTION

By IUPAC definition „biosensor is a device that uses specific biochemical reactions mediated by isolated enzymes, immunosystems, tissues, organelles or whole cells to detect chemical compounds“. They comprise sensitivity and specifity of biological sensing element with physicochemical transducer for accurate detection of a desired analyte. Presently they find application in medicine, pharmacology, food and environment control, but most of the market of over US 25.5 billion is driven by medical diagnostics, in particular glucose sensors for diabetes patients. (Biosensors market report 2021; Turner, 2013).

First presented in 1962 by Leland C. Clark following his invention of Clark oxygen electrode, by immobilising glucose oxidase (GOX) on platinum electrode, he created an analytical device for blood glucose detection and gave rise to the first generation of mediatorless amperometric biosensors. In over 60 years of research, three generations of biosensors have risen and three flavin adenine dinucleotide (FAD) dependent enzymes of the Glucose-methanol-choline (GMC) family were utilized for glucose detection: GOX, glucose dehydrogenase (GDH) and cellobiose dehydrogenase (CDH). Today the development of 3$^{rd}$ generation biosensor is still ongoing, and with the development of nanotechnology and material science, this is expected to deliver highly selective, non-mediated biosensors with improved response time (Zhang and Li, 2004). Despite the setbacks which will be addressed further in the text, this technology still has potential. The second generation utilized unstable mediators and further optimization lead to third generation based on direct electron transfer (DET) from enzyme to electrode. Only the cytochrome domain of CDHs, a member of GMC family, can facilitate DET. CDH from *Basidiomycota* are used for third generation lactose biosensors due to the not so high substrate specificity and CDH from certain *Ascomycota*, with higher catalytic activity towards glucose are used in glucose biosensors (Ma and Ludwig, 2018). Nevertheless, although with an interdomain electron transfer (IET) and DET, CDH catalytically doesn't favor monosaccharides, and therefore isn't suitable for a high selectivity third generation glucose biosensor. GOX is used in first generation sensors, although with high specificity towards glucose had proven to be unstable (Leskovac et al., 2005; Rocchitta et al., 2016) and GDH, which is used in second generation sensors, shares the substrate

specificity with GOX, displays high turnover number and increased stability, but doesn't carry a cytochrome domain, therefore isn't capable of DET (Sygmund et al., 2011; Zafar et al., 2012).

New strategies have been employed for the production of ideal DET capable enzyme, by combining and characterizing these functionalities of FAD-dependent GMCs with the help of genetic and chemical engineering (Zhang and Li, 2004) and this thesis will deal with two of those subjects.

First goal of this thesis was to create recombinant chimeric flavoprotein capable of DET by combining GDH recombinantly expressed in *Pichia pastoris X33,* with cytochrome *c* expressed in *Escherichia coli* via sortase-mediated domain fusion (sortagging) by post-translational conjugation. Sortase A was also recombinantly expressed in *Escherichia coli*, individually.

Second part of this thesis will deal with stability of native GOX and different recombinant FAD-dependent GMCs by examining and comparing the cofactor dissociation constant ($K_D$ value), measured and calculated based on activity assays and fluorescence measurements of deflavinated apoenzymes (with cofactor removed) and reflavinated holoenzymes. Since FAD is not covalently bound, turnover numbers and protein stability decrease if the cofactor is depleted or if the catalytic reaction leads to inactivation of the cofactor. By measuring the $K_D$, the knowledge of the affinity will show if the cofactor depletion over time is a factor to consider. Enzymes analysed in this thesis are native *An*GOX (Sigma Aldrich, St. Louis, Missouri, US) and recombinant: *An*GOX_pps (*An*GOX expressed in *P.pastoris* Superman5), *Gc*GDH, *Mt*-DH (CDH expressed in *Myriococcus thermophilum* without the cytochrome domain), *An*GOX_pps *(P. pastoris X33*) and *Mt*DH from wild type *P.pastoris X33.*

# 2. THEORY

## 2.1. BIOSENSORS

Biosensor is a device which measures biological or chemical reactions by generating signals proportional to the concentration of a desired analyte in the reaction. They are ubiquitous in biomedical diagnosis, in applications such as drug discovery and monitoring of diseases as well as in environmental monitoring and food control (Bhalla et al., 2016). Every biosensor consists of biological recognition element directly interfaced to a signal transducer (Zhang et al., 2004). Transducers can be classified into optoelectric (measuring luminescence, absorption etc.), piezoelectric (mass sensitive measurements) and electrochemical biosensors, the latter being the most predominant. The most common forms of bioreceptors used in biosensing are based on: antibody/antigen interactions (e.g. Radioimmunoassay), nucleic acid interactions, enzymatic interactions, cellular interactions (cells, cellular structures, or non-enzymatic proteins such as cytochromes in the serving as a bioreceptor for intracellular reactions taking place in another part of the cell) and interactions using biomimetic materials (i.e., synthetic bioreceptors) according to Vo-Dinh and Cullum from a review published in 2000.

Enzyme selectivity coupled with the sensitivity of electrochemical detection, operation simplicity, low fabrication expenses and real-time detection make this biosensor type a particularly interesting concept in the field of biotechnology ever since it's proposal by Leland C. Clark, Jr. in 1956 (Zhang et al., 2004; Bhalla et al., 2016). However, this concept has its disadvantages concerning enzyme stability and electrical communication between the two components and until today there were multiple approaches to its optimization.

### 2.1.1. Development of biosensors

#### *2.1.1.1. First generation*

Clark, Jr.'s glucose oxidase based oxygen electrode in which oxygen mediates communication of electrons between enzyme and the electrode gave rise to the first generation of biosensors. They are called mediatorless amperometric biosensors and measure the concentration of analytes and/or products of enzyme reactions that diffuse to the transducer surface and generate an electric response. These biosensors employ cofactor dependent oxidases and dehydrogenases. They have proven to be highly sensitive, with low response times. The idea's popularity has decreased during the years and was outweighed by the disadvantages, such as reduction of

detection limit due to prolonged use especially in complex biological matrices or undiluted samples, by fouling of the transducer's surface. Measurements often required electrode pretreatment to generate reproducible response (Bhalla et al., 2016; Rocchitta et al., 2016).

*2.1.1.2. Second generation*

Second generation of biosensors exploits mediators (most commonly ferricyanide and ferrocene, although, methylene blue, phenazines, methyl violet, alizarin yellow, Prussian blue, thionin, inorganic redox ions are also used) as oxidizing agents. Mediators can be added to the sample or immobilized on the electrode surface, but should be entrapped close to the enzyme. These biosensors are less commonly used than first generation on the grounds of low stability due to immobilized mediators, but mostly because they have to be operated usually at high potentials and are therefore prone to interferences.

*2.1.1.3. Third generation*

The need for third generation of biosensors occurred due to the disadvantages of mediated glucose sensors. The nature of the biochemical structure of glucose oxidase enzyme, relative solubility and toxicity of mediators and generally poor stability of these mediated biosensors towards continuous use lead researchers to a new approach, sensors based on direct electron transfer between the enzyme redox center and the electrode (Juska and Pemble, 2020). Third generation biosensor consists of three elements: enzyme as bio-recognition element, redox polymer for signal propagation and the electrode as the entrapping surface. These biosensors rely on bioelectrocatalysis with direct electron transfer between enzyme and electrode. These biosensors are still under development and with advances in material science and nanotechnology should be proven useful, highly selective and with improved response time. Their main advantage is absence of mediators and consequently superior selectivity due to working conditions closer to the enzyme's redox potential and lack of another substance in the reaction. Another advantage is the opportunity to customize protein to our own needs by means of genetic and chemical engineering (Degani and Heller, 1987), which is one of the strategies to tackle the problematic of achieving direct electron transfer (DET). DET is the main "bottleneck" for third generation biosensor development, since not many enzymes are capable of direct electron transfer to the normal electrode surfaces. Extensive studies are being carried out to

develop novel surface functionalization, electrode materials and enzymes so DET could be achieved. (Bhalla et al., 2016; Rocchitta et al., 2016.)

This thesis will discuss the new approaches by genetic and chemical engineering to third generation biosensor development, including enzyme modifications in order to produce DET-capable enzyme by recombinant production of chimeric enzyme. Furthermore, taking into the account the widespread use of glucose oxidase (GOX) in biosensors, it will characterize some members of the Glucose-methanol-choline (GMC) superfamily of oxidoreductases, in which glucose oxidase (GOX) belongs to.

## 2.2. GMC FAMILY OF OXIDOREDUCTASES

Glucose-methanol-choline (GMC) superfamily of oxidoreductases was first defined by Caverner in 1992 based on the sequence similarities of flavoenzymes including glucose dehydrogenase from *Drosophila melanogaster*, methanol oxidase from yeasts *Hensenula polymorpha* and *Pichia pastoris*, glucose oxidase from *Aspergilus niger* and choline dehydrogenase from *Escherichia coli*. They occur in yeasts, filamentous fungi (*Ascomycetes, Basidiomycetes*), bacteria, insects or plants. Although they use different substrates ranging from various sugars and alcohols to choline and cholesterol, they share similar reaction mechanisms due to their shared flavin adenin dinucleotide (FAD) binding domain containing typical Rossman fold or βαβ mononucleotide-binding motif. Substrate binding domain varies structurally depending on the preferred substrate (Levasseur et al., 2014; Sützl et al., 2019).

Depending on the His/His or His/Asn pair in the active site, reaction mechanism can be separated on a reductive half reaction (reduction of FAD associated by substrate (electron donor) oxidation) and an oxidative ($FADH_2$ reoxidation) half reaction. Based on the electrone acceptor preferences, GMCs that employ $O_2$ as electrone acceptor fall into oxidases, and those which utilize different quinones, phenol radicals or metal ions are classified as dehydrogenases (Sützl et al., 2019).

### 2.2.1. CAZy AA3 family

Fungal GMC oxidoreductases, oxidizing alcohol and sugars are practically aplied in biomass utilization and mostly used in biosenzors in food industry due to their displayed auxiliary roles in lignocellulose degradation. Therefore they are summarized in the AA3 family of „Auxiliary

Activities“ (AA) class of Carbohydrate-Active enZyme (CAZy) database (http://www.cazy.org/Auxiliary-Activities.html). CAZy database describes enzymes and their domains which degrade, modify or create glycosidic linkages. AA class enzymes act in conjuction with CAZymes. AA3 family's main representatives are aryl-alcohol oxidoreductase, pyranose oxidase, alcohol oxidase, glucose oxidase, cellobiose dehydrogenase and glucose dehydrogenase, all of which are FAD dependent (Levasseur et al. 2013; Sützl et al., 2018). The last three are characterized in this thesis.

*2.2.1.1. Glucose oxidase (GOX)*

Glucose oxidase (β-d-glucose:oxygen 1-oxidoreductase, EC 1.1.3.4) catalyzes the oxidation of β-d-glucose by molecular oxygen to glucono-δ-lactone, which subsequently hydrolyzes spontaneously to gluconic acid and hydrogen peroxide (Wilson and Turner 1992; Leskovac et al., 2005). Hydrogen peroxide and δ -gluconolactone both break down spontaneously and catalytically, but accumulation of hydrogen peroxide by itself and the accumulation of breakdown product of δ -gluconolactone, gluconic acid ($C_6H_{12}O_7$) which subsequently reduces the pH of the solution, can result in product inhibition of GOX (Wong et al., 2008). Along with the GDH it falls into AA3_2 family in the CAZy database (Levasseur et al., 2013).

GOX was first discovered by Muller in 1928 in *Aspergillus niger* extracts. By today, DNA sequence of the GOX gene had been determined and published (Kriechbaum et al., 1989). Structurally it is a homodimer made of two identical 80-kDa subunits and two non-covalently bound FAD cofactors, which act as electron carriers during catalysis (Wilson and Turner, 1992). It is currently best characterized glucose oxidase and predominantly used in industrial applications (Wong et al., 2008).

GOX is capable of oxidizing monosaccharides, nitroalkanes and hydroxyl compounds, but its activity towards substrates other than glucose is low. As electron acceptor, naturally dissolved oxygen gives the highest enthalpy, other potential electron acceptors, such as quinones have lower redox potential than $O_2$ and therefore lower reaction rate. (Leskovac et al., 2005).

*2.2.1.2. Cellobiose dehydrogenase (CDH)*

The first subfamily of the AA3 family (AA3_1) consists of cellobiose dehydrogenases (CDH; EC 1.1.99.18, cellobiose:acceptor 1-oxidoreductase) (Levasseur et al., 2013), which are to date

the only known extracellular hemoflavoproteins. It was first discovered and described by Eriksson and co-workers while analyzing the secretomes of the white-rot fungi *Trametes versicolor* and *Phanerochaete chrysosporium* in the presence of cellulosic substrates (Westermark and Eriksson 1974).

CDH is a monomeric multi-domain glycoprotein with FAD and haem *b* cofactors, at N-terminal cytochrome ($CYT_{CDH}$) and the C-terminal dehydrogenase ($DH_{CDH}$) domain. The CYT domain has been classified as a separate auxiliary activity in the CAZy database as AA8 of iron reductases (Levasseur et al., 2013).

CDHs oxidise cellobiose, cellodextrins or structurally related oligosaccharides, such as lactose at C-1 of the reducing end. Cellobiose is oxidised to cellobiolactonate, which spontaneusly hydrolyses to cellobionate, while FAD is reduced to $FADH_2$. CDHs show low catalytic efficiency towards monosaccharides, but oxidise hemicellulose and starch derived oligosaccharides. As a result of a reductive half reaction, two electrones taken up by the $DH_{CDH}$ domain can be transferred to either two eletron acceptor, such as DCIP (2,6-dichloro-indophenol) or one electron acceptor, such as heam *b* group in $CYT_{CDH}$ domain which then reduces a terminal electron acceptor, such as copper in LPMOs or other complexed metal ions e.g. $Fe^{3+}$ or $Mn^{3+}$ malonate (Sützl et al., 2018). CDH is the most suitable and one of the best documented biorecognition element for third generation DET-based biosensors thanks to the interdomain electron transfer (IET) within CDH and DET to electrodes (Ludwig et al., 2010; Ma and Ludwig, 2018).

*2.2.1.3. Glucose dehydrogenase (GDH)*

Phylogenetically and catalically closely related to GOX, FAD dependent GDH (EC 1.1.99.10) is also a part of AA3_2 family, but hasn't been initially included in the original description of AA3_2 (Levasseur et al., 2013). It was first discovered in *Aspergillus oryzae* in 1951, but hasn't been noticed until the utilization of FADGDH as electrode catalyst for glucose biosensors and biofuel cell anodes had been promoted. After that, new members were identified from the fungi *A. terreus* and *A. oryzae and Penicillium lilacinoechinulatum.*

Recently a new FAD-dependent GDH has been discovered from *Glomerella cingulata* (*Gc*GDH). Native enzyme is a monomeric glycosylated polypeptide with one non-covalently bound FAD molecule acting as a redox cofactor. Two other types of GDHs were utilized for

glucose based biosensors and biofuel cells, GDH with a pyrroloquinoline quinon as a bound cofactor (PQQGDH) and nicotine adenine dinocleotide (NAD) dependent GDH. Thermostabile FADGDH has turned out to be most suitable for glucose biosensors due to high turnover rates, substrate selectivity, good stability and lower redox potential than that of PQQGDHs and an oxidative half reaction of the reduced FAD unaffected by oxygen. (Sygmund et al., 2011; Zafar et al., 2012).

## 2.3. STRATEGIES EMPLOYED IN THE DEVELOPMENT OF THE THIRD GENERATION BIOSENSORS

### 2.3.1. Recombinant production of chimeric enzymes capable of DET

Gene expression tools are utilized to produce an enzyme which meets industrial needs and presents properties such as stability over a wide range of of pH and temperature, high specific activity and resistance to cations (Potvin et al., 2012). In this particular case, DET function is crucial to mimic natural processes occuring in multidomain enzymes already used in third generation biosensors, such as CDH. An increased DET is subsequently paired with higher turnover numbers, higher specific currents, lower detection limits and higher sensitivies.

DET, or direct electron transfer between oxidoreductases and an electrode occurs rarely in enzymes because they have usually buried redox center and it takes place between their active-site cofactor an electrode, whereas other oxidoreductases depend on and acquired cytochrome domains as built-in redox mediators. DET was discovered in 1973 by Yeh and Kuwana as well as Eddows and Hill for cytochrome *c*, and in 1980s first flavocytochrome $b_2$ based biosensor without soluble redox mediator was developed, showing that a cytochrome domain can work as an internal electron transfer (IET) unit in oxidoreductases. To achieve high IET and DET rates and consequently, high current density for glucose biosensors, good interaction of the cytochrome with the active-site cofactor should be achieved. (Ma and Ludwig, 2018).

#### *2.3.1.1. Cytochromes*

Cytochromes are ubiquoitusly found in muscles, tissues and organs of vertebrate and invertebrate animals as well in all kinds of bacteria. They carry a respiratory function as specific electron

acceptors or donors of the mitochondrial electron transfer chain and have other functions, such as storage of electrons for homeostasis maintanance in redox environment and have evolved specific protein interfaces for the purpose of redox partners recognition and facilitation of fast electron transfer.

Current cytochrome classification into six classes: *a*, *b*, *c*, *d*, *f* and *o* is based on their different absorption bands. The difference of these cytochromes is in the chemical substituents of the haem tetrapyrrole ring, it's linkage to protein, or both. Cytochromes *b* and *c* can be found assingle cofactor proteins and in complexes, e.g. multi-cofactor enzymes. In cytochrome *c*, haem tetrapyrrole ring is covalently attached via two thioether bonds to the cysteine residues of the protein's binding pocket, which is not the case for the haem *b*. The best studied cytochrome, and the model protein for DET studies in electrochemistry is cytochrome *c* (Ma and Ludwig, 2018).

*2.3.1.2. Sortagging of a chymeric enzyme*

Sortase-mediated transpeptidation (sortagging) is the method for promotion of domain fusion in chimeric proteins by post-translational conjugation via site-specific labeling of proteins.

Bacterial sortases are thiol-containing enzymes that covalently attach proteins to the bacterial cell wall. Sortase A of *Staphylococcus aureus* recognises an LPXTG motif on different substrates and cleaves the motif's peptide bond between threonine and glycine (Popp et al., 2007). Cleavage between the threonine and the glycine of the LPXTG motif liberates the carboxyl of threonine to form an amide bond with the amino group of the pentaglycine crossbridge, thereby tethering the C-terminus end of surface proteins to the bacterial peptidoglycan (Navarre and Schneewind, 1994). In 2007, Popp et al., have succesfully exploited the transpeptidase activity of sortase A for selective labeling of proteins in solution, in cell lysates and on the surface of the living cells with a diverse set of readily synthesized probes suitable for protein interactions and trafficking study.

In the first part of this thesis, sortase A was expressed in *E. coli*. After purification it was used for sortagging assay. Sortase A cleaved LPETG motif on cytochrome c (also individually expressed in *E. coli*), between threonine and glycin, to form an amide bond between threonine and glycins on GDH (previously recombinantly expressed in *P. pastoris X33*), thus forming cytochrome-LPET--G-GDH chimeric complex capable of DET.

2.3.2. Chemical method of enzyme modification: cofactor dissasociation and association

Flavoenzymes typically contain either a flavin mononucleotide (FMN) or a flavin adenine dinucleotide (FAD) cofactor, both of which are synthesized *in vivo* from riboflavin, i.e., vitamin B2. Their stuctures are shown in Figure 1. Flavins are the main components of GMC oxidoreductases as they serve as prosthetic groups, lending their redox capability to the holoenzyme. In most of the flavoproteins, flavin is tightly but not covalently bound with a dissociation constant $K_D<10^{-10}$ M. However, in a subset of them (ca. 10%), the flavin is mono- or bicovalently attached to the polypeptide chain and in these cases, it has been observed that the covalent flavin allows catalysis of more thermodynamically challenging reactions by modulating the cofactor redox potential (LudwigLab, 2018; Posthuma-Trumpie et al., 2007; Romero et al., 2018).

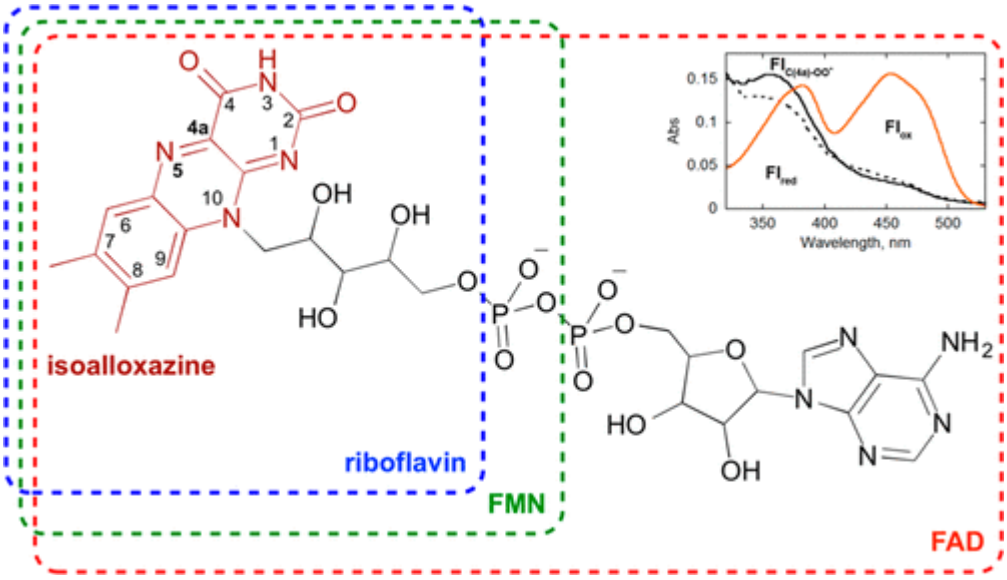


**Figure 1**. Structures of flavin mononucleotide (FMN) and flavin adenine dinucleotide (FAD) cofactors, derived from riboflavin. (Inset) UV–vis absorption spectra of the oxidized, two-electron reduced, and C(4a)–peroxyflavin (orange, black broken, and black lines, respectively) (adapted from Romero et al., 2018)

The binding of flavins to proteins is facilitated by the evolution of different flavin folds, and specific parts of flavin molecule are recognized within structural motifs, such as Rossman fold (Hefti et al., 2003). As many other cofactor-dependent proteins, flavoproteins often fold in vivo

in cellular environments where their cognate cofactors are present, thus binding to the appropriate polypeptide before folding. It is possible that cofactor serves as the nucleation site facilitating the overall folding process (Caldinelli et al., 2008).

FAD dissociation directly leads to activity loss and apoenzyme destabilization, compromising the applicability of flavoenzymes in biosensing purposes. Covalent binding of the FAD to the protein would prevent dissociation, but currently employed synthetic or genetic methods affect the stereochemistry and therefore catalytic and redox properties (LudwigLab, 2018).

Deflavination and reconstitution give a valuable insight in protein folding, function and mechanism. Replacement of the natural cofactor with a synthetic analog has been especially useful for determination of the solvent accesibillity, polarity, stereochemistry and dynamic behaviour of active sites (Hefti et al., 2003). Preparation of the apoenzyme is carried out under harsh conditions, partial unfolding occurs under extremely acidic pH values and in the presence of high salt concentrations (Swoboda et al., 1964), or in neutral to slightly basic environment with high salt concentration. Removal of flavin can be performed by size exclusion cromatography or ultrafiltration. Prepared apoenzyme still maintains low residual activity (Posthuma-Trumpie *et al.,* 2007; Garajova et al., 2017).

To characterize the affinity of apoenzyme to synthetic FAD flurimetric measurements were conducted by titration of stock FAD solution to the apoenzyme. Based on the fluorescence spectra we were able to calculate $K_D$ values of native *An*GOX (Sigma Aldrich, St. Louis, Missouri, US) and recombinant: *An*GOX_pps (*An*GOX expressed in *P.pastoris* Superman5), *Gc*GDH, *Mt* DH (CDH expressed in *Myriococcus thermophilum* without the cytochrome domain), *An*GOX_pps *(P. pastoris X33*) and *Mt*DH from wild type *P.pastoris X-33,* obtained from institute culture collection. The *Mt*DH in this study represents the *Mt*DH variant N700S/N748G (Oxy +), which has higher turnover numbers for both oxygen and cellobiose. 3D models of recombinant enzymes are shown in Figure 2.

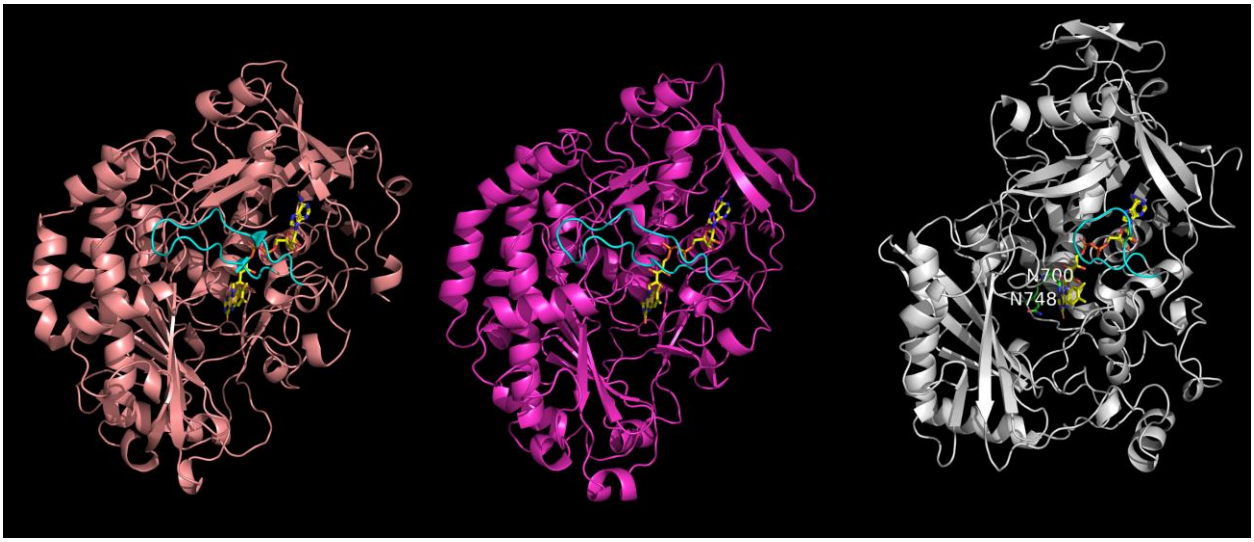


**Figure 2.** 3D models of studied GMCs by the order of appereance: 1. *An*GOX_*pps*, *Gc*GDH, *Mt*DH N700S/N748 with representation of spatial orientation of FAD cofactor (yellow) and the loop motif (cyan) covering the FAD binding site. The active site and the entrance channel for the substrate is located in the south of isoaloxazine ring.

# 3. EXPERIMENTAL PART

## 3.1. CHEMICALS AND MEDIA

### 3.1.1. Chemicals

All chemicals used in these experiments were of analytical or higher grade purity and were obtained from Sigma Aldrich (St. Lous, Missouri, USA), New England Biolabs Inc. (Ipswich, Essex County, Massachusetts, USA), Carl Roth (Karlsruhe, Germany), PanReac Applichem (Chicago, Illinois, USA) or Fluka (Vienna, Austria).

New England Biolabs Inc. kits were used for the purposes of plasmid preparation, purification, ligation and digestion of DNA fragments. NEB kits contained pre-prepared buffers, columns and protocols, which were respectfuly followed to obtain the best results.

### 3.1.2. Media

#### *3.1.2.1. Media for Escherichia coli*

- Standard LB (Luria Broth) media contains:
  - 10 g $L^{-1}$ of Peptone From Casein
  - 5 g $L^{-1}$ of Yeast Extract
  - 10 g $L^{-1}$ of NaCl
  - (15 g $L^{-1}$ Agar-agar (for plating))

- Low salt LB (Luria Broth) media contains:
  - 10 g $L^{-1}$ of Peptone From Casein
  - 5 g $L^{-1}$ of Yeast Extract
  - 5 g $L^{-1}$ of NaCl
  - (15 g $L^{-1}$ Agar-agar (for plating))

LB media contains all necessary nutrients for optimal growth of *E. coli*. Media was autoclaved at 121°C for 15 min and cooled to 60°C in water bath before use. Transformed cells carrying

antibiotic resistance gene were selected by addition of 100 mg $L^{-1}$ Ampicillin and/or Chloramphenicol after media was cooled.

- SOC media (Super optimal broth with catabolite repression) medium (New England Biolabs, Ipswich, USA) contains:
    - 20 g $L^{-1}$ of Vegetable Peptone
    - 10 g $L^{-1}$ of Yeast Extract
    - 20 mM Glucose
    - 2.5 mM KCl
    - 10 mM NaCl
    - 10 mM $MgCl_2$
    - 10 mM $MgSO_4$

*3.1.2.2. Media for Pichia pastoris X-33*

- Standard YPD (Yeast Extract Peptone Dextrose) media contains:
    - 20 g $L^{-1}$ of Peptone
    - 10 g $L^{-1}$ of Yeast Extract
    - 4 g $L^{-1}$ of Glucose
    - (15 g $L^{-1}$ Agar-agar (for plating))

YPD media was autoclaved at 121°C for 15 min and cooled in water bath to 60°C before use.

## 3.2. PRODUCTION OF THE CHIMERIC ENZYME

### 3.2.1. Transformation of plasmid in *Escherichia coli*

Transformation was carried out following "High Efficiency Transformation Protocol" obtained from New England Biolabs Inc.

50 µl of chemically competent NEB-5 alpha *E. coli* cells (acquired from New England Biolabs Inc.) was first thawed on ice for 10 minutes. 1 µl containing 100 ng of plasmid DNA was then added to the cell mixture. The tube was flicked 4–5 times to mix cells and DNA and was placed on ice to incubate. After 30 minutes of incubation the suspension was subjected to heat shock treatment at exactly 42°C for exactly 10 seconds on a preheated thermo mixer, without mixing. The cells were then placed on ice for 5 minutes. 950 µl of 37 °C SOC media was pipetted into

the mixture and placed at thermo mixer set at 37°C and 250 rpm. After 60 minutes of incubation, 100-200 µl of cell suspension was plated on one petri dish with LB medium and Ampicillin as selection marker, preheated at 37°C and the rest of the suspension on other petri dish under the same conditions. Only Ampicillin resistant cells were able to grow on plates as shown in Figure 3**.**

Identical procedure was performed with BL21 cells (acquired from New England Biolabs Inc.)

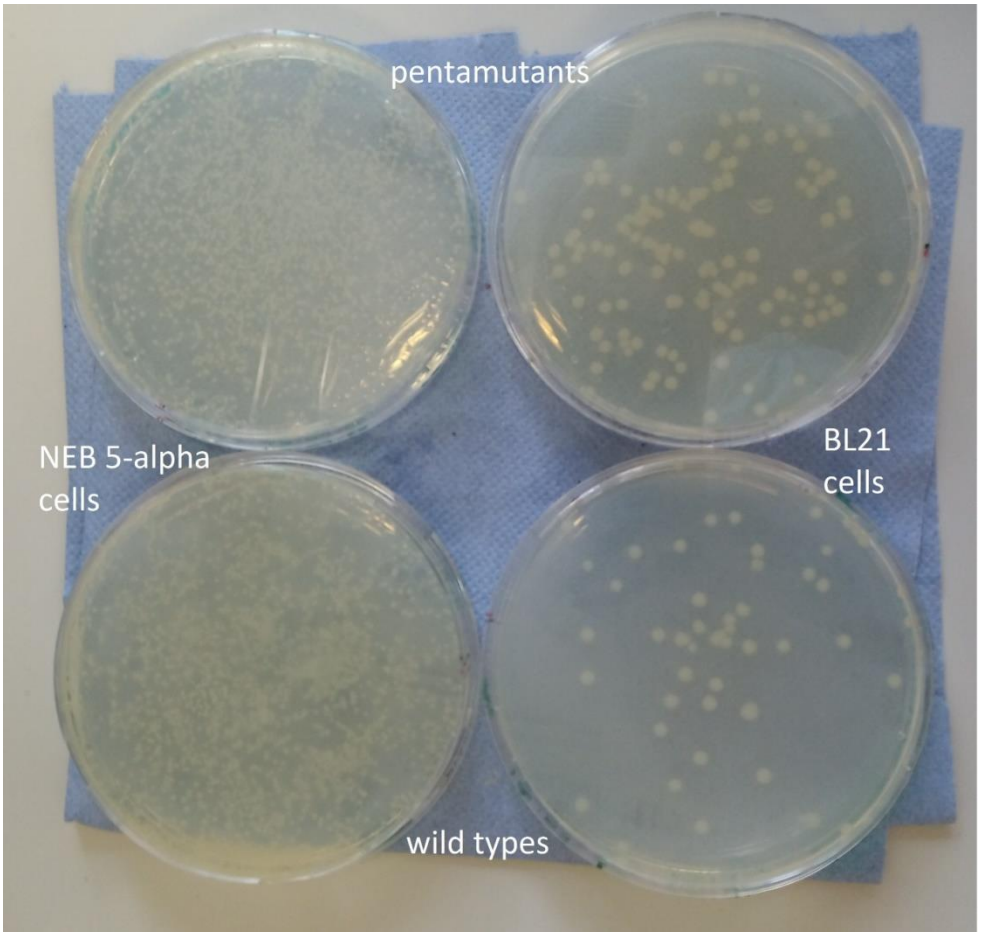


**Figure 3.** Successfully transformed NEB 5-alpha and BL21 *E. coli* wild type and pentamutants on LB plates with Ampicillin

### 3.2.2. Plasmid preparation

The protocol, buffers and the equipment for plasmid preparation, e.g. “Monarch Plasmid Miniprep Protocol” was obtained from New England Biolabs Inc. and was carried out

accordingly, except we used water instead of elusion buffer.

1-5 ml of bacterial culture with less than 15 OD units was centrifuged at 16000 g for 30 seconds. Bacterial culture pellet was resuspended in 200 µl of Plasmid Resuspension Buffer. The suspension was then vortexed until full resuspension of cells was achieved. 200 µl of Plasmid Lysis Buffer was added and the suspension was left for incubation at room temperature for 1 minute. Change in color occurred from dark pink to transparent and suspension became viscous. After mixing with 400 µl of Plasmid Neutralization Buffer, color changed to yellow and precipitate formed followed by RNA removal by RNase A by centrifugation of lysate at 16000 g for 5 minutes. A compact pellet was discarded, and supernatant was carefully transferred to the spin column and centrifuged at mentioned speed for 1 minute. The flow through was discarded and plasmid was captured on the resin of the spin column. The spin column was then inserted into collection tube and washed with 200 µl of Plasmid Wash Buffer 1 and centrifuged for 1 minute, then washed again in 400 µll of Plasmid Wash Buffer 2. Removal of the plasmid from the column was achieved by addition of 30 µl water and centrifugation for 1 more minute.

The concentration of plasmid was then measured with NanoDrop 2000 Spectrophotometer (Thermo Fisher Scientific, Waltham, Massachusetts, USA) by absorption at 260 nm and the sample of satisfactory purity and concentration was sent to an external company for Sanger sequencing to determine if the desired DNA sequence has actually incorporated into plasmid without mutations and in the correct reading frame.

3.2.3. Restriction digestion of gene fragments and ligation

Protocols and restriction enzymes for digestion and ligation of vector and gene were obtained from New England Biolabs.

Digestion was carried out in 20 µl reaction mixes.

1 µl of EcoRI-HF was mixed in the first Eppendorf tube with 1 µl NcoRI-HF, 2 µl of CutSmart (10x concentrated) buffer and 10 µl of gene of interest in a concentration of ~250 ng $ml^{-1}$, when the reaction was finished it was diluted with 6 µl of HQ water to a final volume of 20 µl.

1 µl of EcoRI-HF was mixed in the second Eppendorf tube with 1 µl NcoRI-HF, 2 µl of CutSmart (10x concentrated) buffer and 2 µl of the respective plasmid (pET-21a for the sortase A gene and pET-22b for the cytochrome), when the reaction was finished it was diluted with 13 µl of HQ to a final volume of 20 µl. Both reactions were incubated for 20-30 min at 37°C. Then

another incubation was performed in a thermomixer at 80°C for another 20 minutes.
Then they were cooled on ice so the concetrations in both tubes would return to the starting value (because of water condensation during the last incubation).
Using NEB Ligation calculator, importing length of insert and vector in base pairs, we got the desired insert DNA mass for optimal ratio.
Ligation reaction in 1,5 ml Eppendorf tube was achieved by mixing 2 µl of T4 DNA ligase with 2 µl of T4 DNA ligase buffer (10x), 1 µl of vector (corresponds to 20 ng of gene), 1 µl of insert (gene) with 14 µl water to a final volume of 20 µl. The ligation mix was then incubated for 15 minutes at room temperature. Insert is then added to cells for the transformation. Cells are plated on Petri dishes with LB medium with Ampicillin and only transformed cells will grow on plates.

### 3.2.4. Sortase A production and purification

#### *3.2.4.1. pET-21a(+) vector*

The pET-21a (+) vector carries an N-terminal T7-Tag sequence plus an optional C-terminal His-Tag sequence. This vector carries selectable marker Ampicillin resistance cassette selection marker.

#### *3.2.4.2. Protein expression in shaking flasks E. coli culture*

Fresh LB medium was inoculated with 1% v/v overnight culture incubated 37°C on a shaker.
Optical density of shaking flasks culture was measured against nonfermented LB media.
Starting optical density of shaking flasks culture was 0.1 and after 20 minutes it was measured again and the value was 0.2. When optical density of shaking flask culture measured by spectrophotometer at 600 nm reached 0.4, after 30 minutes at 37°C, 2250 ml of LB media with grown culture was placed on an Infors Unitron shaker at 25°C for protein expression and 1 µl $ml^{-1}$ (500 mM) IPTG was added to induce protein expression.

#### *3.2.4.3. Cell harvest and affinity chromatography over $Ni^{2+}$ HisTrap column*

The recombinant sortase A pentamutant cells were harvested and pelleted by centrifugation on 10 000 rpm, 4°C for 20 min on Beckman Coulter centrifuge (Brea, California, United States) with JA-10 rotor. The cells were washed from media with Buffer A and centrifuged again on 10

000 rpm, 4°C for 20 min on Beckman Coulter centrifuge with JA-10 rotor. The cell pellet was again resuspended in 4-6 ml Buffer A per g of pellet and frozen at 80°C until further processing. Cells were then thawed on ice and lysed in French press and cell debris was removed by centrifugation.

After vacuum filtration, 80 mL of supernatant (crude extract) was further purified with affinity chromatography using Äkta Explorer (Pharmacia, Sweden) on 5 ml $Ni^{2+}$ HisTrap column (GE Healthcare, USA) under conditions given in Table 1. Immobilized $Ni^{2+}$ cations on HisTrap column selectively bind histidine residues of histidine tag on produced sortase A protein.

Supernatant diluted in buffer A was loaded onto the column until the signal for protein absorption at 280 nm was no longer present. Absorption was monitored over UNICORN™ 7 control software. The flowthrough was analysed with SDS page electrophoresis to determine the efficiency of affinity cromatography. The column was washed with Buffer A (composition is given in the Table 1). The elution of bound protein was carried out in linear gradient from 0 to 100% buffer B (composition is given in the Table), and the protein was eluded at 20% Buffer B concentration, since imidazole has better affinity for $Ni^{2+}$ and therefore pushes out the protein. 1 ml peak fractions with an absorbance at 280 nm were pooled and and further purified.

**Table 1.** Affinity chromatography conditions and specifications

| | |
|---|---|
| Column material | Highly cross-linked spherical agarose, 6% (GE Healthcare, USA |
| Column volume | 5 ml |
| Flow rate | 5.0 m/min |
| Elusion flow rate | 1.0 m/min |
| Buffer A | 20 mM Tris-Hcl<br>500 mM Nacl |
| Buffer B | 20 mM Tris-Hcl<br>500 mM NaCl<br>200 mM imidazol |
| Gradient | 1-100% Buffer B |

*3.2.4.4.Centrifugal microfiltration*

1 ml fractions which showed absorption at 280 nm and therefore contained protein, which was eluted at 20% Buffer B were collected, mixed together and subjected to centrifugal ultrafiltration on 4000 rpm in Amicon Ultra-2 Centrifugal Filters for
DNA and Protein Purification and Concentration (Millipore, Burlington, Massachusetts, USA) with a molecular weight cut-off (MWCO) of 30 kDa in several rounds. After each round they were rebuffered in Buffer A and flowthrough was discarded until protein concentration reached desired value. 25µl of the sample will then be qualified on SDS-PAGE electrophoresis.

3.2.5. Cytochrome production and purification

*3.2.5.1. pET-22b(+) vector*

The pET-22b(+) vector (Cat. No. 69744-3) (Novagen, Merck Group, Darmstadt, Germany) carries an N-terminal pelB signal sequence (66 bp), for potential periplasmic localization, plus C-terminal His Tag sequence, which will be needed in further purification).

*3.2.5.2. Cytochrome expression in shaking flasks E.coli culture*

3 liters of fresh LB medium with 100 µl/ml of Ampicillin and 100 µl/ml Campicillin distributed in 12 Erlenmayer flasks was inoculated with 1 % v/v of BL21 *E.coli* cells transformed with 3A9f cytochrome *c* overnight culture incubated at 37°C. Shaking flask culture was then incubated on a shaker at 37°C until optical density reached 0.4. For protein expression induction 100 µl/ml IPTG was added, and inoculated medium was left for overnight cytochrome expression at 25°C.

*3.2.5.3. Periplasmic shock*

The recombinant culture with fermented LB medium was harvested and pelleted by centrifugation on 10 000 rpm, 4 °C for 15 min on Beckman Coulter centrifuge (Brea, California, United States) with JA-10 rotor. The pellet was then resuspended carefully in 200 ml of 20 % Tris Sucrose buffer (50 mM Tris base, 20 % sucrose, pH 7.5) at room temperature to induce

periplasmic shock. The suspension was then pelleted by 10 000 rpm centrifugation at 4 °C for 15 min on Beckman Coulter centrifuge with JA-10 rotor.

*3.2.5.4. Osmotic shock*

The wet biomass was resuspended on ice in 200 ml of 5 mM $MgSO_4$ and left to incubate 15 min to induce osmotic shock, which would lead to cytochromes expressed in periplasmic space being released from cells in supernatant.

Pink pellet was sonicated to lyse the cells, so the residual cytochromes which didn't get extracted to periplasmic space would get extracted into liquid phase. Lysate was then filtered over a vacuum pump to remove debris and loaded to the DEAE sepharose chromatography column for ion exchange.

*3.2.5.5. Affinity chromatography over $Ni^{2+}$ HisTrap column*

250 ml of crude extract, supernatant, or periplasmic fraction was then rebuffered in Buffer A (composition given in the Table 3), filtered over vacuum pump and loaded onto 35 ml $Ni^{2+}$ HisTrap column with flow rate of 10 ml/min and fractioned using Äkta Explorer (Pharmacia, Sweden) under conditions given in Table 2 and as shown in Figure 4. Supernatant diluted in Buffer A was loaded onto column until signal for absorption at 280 nm was no longer present. Absorption was monitored over UNICORN™ 7 control software.

Bound cytochromes were then eluded from the column with Buffer B in linear gradient.

1 ml protein fractions eluded were collected and intensively rebuffered in Sortagging buffer (50 mM Tris-HCl, 150 mM NaCl, 10 mM $CaCl_2$) pH 4.0 to reoxidize cytochromes and to remove imidazole.

**Table 2.** Affinity chromatography conditions and specifications

| | |
|---|---|
| Column material | Highly cross-linked spherical agarose, 6% (GE Healthcare, USA |
| Column volume | 35 ml |
| Flow rate | 10 ml/min |
| Buffer A | 10 mM Tris-HCl, |

| | |
|---|---|
| | pH 7 |
| Buffer B | 10 mM Tris-HCl<br>500 mM NaCl,<br>pH 7 |
| Gradient | 1-100% Buffer B |


**Figure 4.** Cytochrome purification on Äkta Explorer (Pharmacia, Sweden) over $Ni^{2+}$ HisTrap column

*3.2.5.6. Microfiltration of fractions*

Cytochrome fractions pooled together and repeatedly rebuffered in Buffer A to remove imidazole and reoxidize cytochromes then microfiltrated at 4000 rpm in Amicon Ultra-2 Centrifugal Filters with a molecular weight cut-off (MWCO) of 30 kDa until satisfactory concentration was achieved. Cytochrome samples were then stored at 4°C for Size exclusion which will follow.

*3.2.5.7. Size exclusion of apocytochromes from cytochromes over Superdex 75 column*

Heme loaded cytochromes were separated from the apocytochromes using Superdex 75 column on Äkta Pure system (GE Healthcare Bio-Sciences, Pittsburgh, Pennsylvania, USA) with a flow rate of 0,75 mL $min^{-1}$, with the PBS buffer (10 mM phosphate buffer, 140 mM NaCl, pH 7.4) as an elusion buffer.

3.2.6. Sortagging of the chimeric enzyme

*3.2.6.1 Sortagging assay*

*Gc*GDH was recombinantly produced in *Pichia Pastoris X-33* on YPD media and purified by other lab members.

Cytochrome and *Gc*GDH samples were rebuffered in Sortagging buffer of (50 mM Tris-HCl; 150 mM NaCl; 10 mM $CaCl_2$) with a pH value of 4.0.

Sortagging reaction was performed in Amicon tube with a molecular weight cut-off (MWCO) of 30 kDa by mixing cytochromes and GDH in a ratio 5:1 followed by addition of sortase A in 1:10 ratio compared to GDH. The mix was then incubated for 3 h at 30 °C in 20 ml Amicon tube. During the incubation period, sortase A cleaves improved LPETG motif between T and G on cytochrome *c* and binds it to Glycins present on *Gc*GDH, thus forming peptide bond between the two parts of chimeric enzyme. Assay was performed in a centrifuge so the G-tags (glycins) pass to the supernatant and the LPETG motif on cytochrome *c* wouldn't again be connected to the G-tags (which were cleaved by the sortase A).

*3.2.6.2. Purification of chimeric enzyme by cation exchange chromatography over HisTrap/Mono S™ column*

When sortagging reaction was finished, total volume of the reaction was rebuffered 10 times in 50 mM Tris buffer (pH 4.00) in 1:10 ratio and loaded to HisTrap column with a 100 µl sample loop, since the volume was small (300 µl). HisTrap and Mono S columns were connected as shown in Figure 5 and the purification was performed under the conditions given in Table 3 and 4 on Äkta Pure system (GE Healthcare Bio-Sciences, Pittsburgh, Pennsylvania, USA) with flow speed of 0.5 ml /min. Buffer B was used as an elusion buffer and the elusion was conducted intensively until pH became stable again, to make sure all unbound protein was removed. Non-

reacted GDH was contained in the flowthrough and thus was kept. Next, Histrap column was disconnected and sample was loaded to 15 ml Mono S™ column for Cation exchange chromatography (Cyativa, Marlborough, MA) in a Buffer B gradient from 1-100% B in 15 column volumes for 160 min.

The eluate containing cytochrome that has lost the HisTag and the chimera was intensively rebuffered in 50 Mm KPP buffer pH 6,00 to remove unbound cytochromes.

**Table 3.** $Ni^{2+}$ His trap Affinity chromatography coupled with conditions and specifications

| | |
|---|---|
| Column material | Highly cross-linked spherical Agarose, 6% (GE Healthcare, USA |
| Column volume | 35 ml |
| Flow rate | 0.5 ml/min |
| Buffer A | 50 mM Tris<br>pH 4.0 |
| Buffer B | 10 mM Tris-HCl<br>500 mM NaCl,<br>pH 4.0 |
| Gradient | 1-100% Buffer B in 5 column volumes |

**Table 4.** Cation exchange chromatography conditions and specifications

| | |
|---|---|
| Column material | MonoS strong cation exchange chromatography resin |
| Column volume | 15 CV |
| Flow rate | 0.15 ml/min |
| Buffer A | 10 mM Tris-HCl<br>pH 7.0 |
| Buffer B | 10 mM Tris-HCl |

| | |
|---|---|
| | 500 mM NaCl,<br>pH 7.0 |
| Gradient | 1-100% Buffer B in 25 column volumes |


**Figure 5.** Purification of chimeric enzyme over Mono S column (left) and $Ni^{2+}$ HisTrap column (right) on Äkta Pure system (GE Healthcare Bio-Sciences, Pittsburgh, Pennsylvania, USA)

*3.2.6.3. Deglycosilation of GDH*

*Gc*GDH was expressed by *Pichia pastoris*, and was posttransationally glycosylated, so it was neccessary to deglycosylate it in order for it to be seen on the SDS gel, otherwise it would be too large for the qualification and the differentiation from the chimeric protein on the SDS gel.

Chemicals and protocol were acquired from New England Biolabs and protocol was followed accordingly.

Aliquot of glycoprotein (chimeric protein) was mixed with 2 µl of 10x GlycoBuffer, 2 µl of PNGase F and was filled up with HQ water until total volume of 20 µl was reached. Reaction was then left for incubation at 37°C for 4 hours .The presence of chimeric protein was then qualified with SDS-PAGE electrophoresis.

### 3.3. $K_D$ DETERMINATION

#### 3.3.1. Enzymes

Enzymes used for determination of $K_D$ values in this thesis were either purchased (native *An*GOx; Sigma Aldrich; St. Louis, Missouri, USA) or were available in the lab and produced recombinantly in *Pichia pastoris X-33* by other lab members (*An*GOx, *Mt*CDH) and in *Pichia pastoris* Superman5 (*Gc*GDH).

#### 3.3.2. Deflavination of GMCs and generation of apoprotein

To determine $K_D$ values of GMCs, apoprotein without the cofactor FAD to be created. By following and adapting the protocol from Swoboda (Swoboda *et al*., 1964) with solutions shown in Table 5. Ammoniumsulfate precipitation was used to deflavinate the GMCs. However, the method slightly differs depending on the enzymes used. Deflavination efficiency was indicated by the decoloration of the resulting protein precipitate.

**Table 5.** Solutions for deflavination

| Solution | Molarity | pH |
|---|---|---|
| Potassium Phosphate (KPP) Buffer | 50 mM | 7.0 |
| Potassium bromide | 3 M | |
| Sodium acetate | 2.5 M | 8.5 |
| Ammonium sulfate | saturated | |

KPP buffer components were calculated from AAT Bioquest webpage. For the preparation of 250 ml of KPP buffer, 1.168 g of $K_2HPO_4$ and 0.789 g of $KH_2PO_4$ was added to 200 mL of dH2O in a suitable container and filled with dH20 until the volume of 250 ml was achieved.
Enzyme solutions were prepared in 50 mM KPP buffer to achieve a concentration of 15-30 mg/ml, taking into the account that the yield of apoprotein rises with higher starting concetration. All the solutions were precooled and fresh.

50 µl of enzyme solution was mixed with equal amount of KBr and added dropwise to the brown 2 ml flask with a saturated $(NH_4)_2SO_4$ solution on ice, while being stirred with a magnetic stirrer. The solution was then transferred to 2 ml Eppendorf tube (Eppi) and centrifuged in a precooled centrifuge at 15000 g at 4°C for 6 minutes. Supernatant containing FAD, indicated by a yellow color was discarded and the pellet was resuspended in 100 µl of 2.5 M NaAc pH 8.5 and a new round of precipitation was started. After a white pellet has appeared no repetition was necessary.
Precipitate was then rebuffered in KPP buffer and amonnium sulfate was removed using a desalting column. Rebuffered apoprotein was transferred to an Eppi and centrifuged at 15000 g for 5 minutes at 4°C. The pellet was transferred to a fresh Eppi, on ice and the concentration was measured in a 3 mm quarz cuvette on a Diode Array spectrophotometer measuring the absorbance at 280 nm.

### 3.3.3. Fluorescence measurements

Proteins are unique in displaying useful intrinsinc fluorescence due to the fluorophores in tryptophan, phenylalanine and tyrosine, with tryptophan being the dominant fluorophore, generally present at about 1 mole % of proteins. A valuable feature of protein fluorescence is the high sensitivity of tryptophan to its local environment with changes in indole ring's surrounding, occurring in response to conformational transitions, subunit association, substrate binding or denaturation. Tryptophan is uniquely sensitive to collisional quenching due to the tendency of electron donation by the excited-state indole, but its emission maximum is not. There are numerous reports on the use of emission spectra, anisotropy, and quenching of tryptophan residues in proteins to study protein structure, folding and function. (Lakowicz, 2006)

By measuring the emitted fluorescence of the cofactor FAD or the Trp residues near the binding site of the FAD the amount of reconstitutable apoprotein was determined. Trp signal is altered by conformational changes due to binding of FAD to the apoprotein. The signal can be measured by excitation at 280 nm and recording the emission between 300 and 400 nm with a peak maximum at ~340 nm. Free FAD can be excited at 280, 380 and 450 nm and emission was visible between 500 and 550 nm with peak maximum at ~525 nm.

Fluorescence measurements have been conducted in Cary Eclipse Fluorescence Spectrophotometer (Agilent Technologies, Santa Clara, California, US) on Figure 6, by series of titrations with FAD stock solutions given in Tables 6 and 7. The same solutions were used for every apoprotein tested. Concentrations of stock solutions were measured on Diode Array Spectrophotometer and calculated based on the molar absorbance coefficient at 450 nm ($\varepsilon_{450}$ = 11.3 $mM^{-1}$ $cm^{-1}$).


**Figure 6.** Cary Eclipse Fluorescence Spectrophotometer (Agilent Technologies, Santa Clara, California, US)

*3.3.3.1. FAD stock solutions*

**Table 6.** Stock FAD solutions for fluorescence measurements

| **Stock FAD concentrations (µM)** | **Final volume (ml)** | **Dilution** | **FAD (µl)** | **Buffer (µl)** |
|---|---|---|---|---|
| 2.5 | 2 | 1:2 | 1000 | 1000 |
| 5.0 | 1 | 1:2 | 1000 | 1000 |
| 10.0 | 1 | 1:2 | 1000 | 1000 |
| 20.0 | 1 | 1:2 | 1000 | 1000 |
| 40.0 | 1 | 1:2 | 1000 | 1000 |
| 80.0 | 1 | 1:2 | 1000 | 1000 |
| 160.0 | 1 | 1:2 | 1000 | 1000 |
| 320.0 | 1 | | | |

**Table 7.** Stock FAD solutions for fluorescence measurements in nM

| **Stock FAD concentrations (nM)** | **Final volume (ml)** | **Dilution** | **FAD (µl)** | **Buffer (µl)** |
|---|---|---|---|---|
| 25 | 1.5 | 1:3 | 500 | 1000 |
| 75 | 1.5 | 1:2 | 1000 | 1000 |
| 150 | 1 | 1:2 | 1000 | 1000 |
| 300 | 1 | 1:2 | 1000 | 1000 |
| 600 | 1 | 1:2 | 1000 | 1000 |
| 1200 | 1 | 1:2 | 1000 | 1000 |
| 2400 | 1 | | | |

*3.3.3.2. Reconstitutable apoprotein*

Not the whole amount of apoprotein generated by deflavination can be reconstituted, and the percentage of reconstitutable protein can be measured by fluorimetry of free FAD at 525 nm

with fluorimeter setup given in Table 8. As a reference, only FAD in KPP buffer was measured and compared to the same concentration of FAD added to the apoprotein.

**Table 8.** Fluorimeter settings for free FAD measurement

| | |
|---|---|
| Excitation | 450 nm |
| Emission | 485-1000 nm |
| Excitation Slit | 10 nm |
| Emission Slit | 20 nm |
| Voltage | 650 V |

Free FAD, as a reference, was measured by addition of 0.4 µM FAD to 2 ml buffer in a quartz cuvette and scanned at 525 nm. Then 0.2 µM apoprotein was added to the cuvette, mixed for 15 minutes in the fluorimeter and scanned again to measure free FAD minus bound FAD. The fluorescence signal intensity at 525 nm (free FAD emission signal) reduces, and that reduction is equivalent to the amount of FAD molecules bound to the reconstitutable apoprotein. To make sure that the ratio between FAD and apoprotein was high enough to measure in a saturating environment, additional 0.4 µM was added. Increase in the signal intensity should be the same as in referent 0.4 µM free FAD cuvette.

After the concentration of reconstitutable apoprotein was determined, $K_D$ was calculated based on the Trp signal, with the fluorimeter setup given in Table 9 and free FAD signal.

*3.3.3.3. Setup for Trp signal*

**Table 9**. Fluorimeter settings for Trp signal

| | |
|---|---|
| Excitation | 280 nm |
| Emission | 330-800 nm |
| Excitation Slit | 5 nm |
| Emission Slit | 5 nm |
| Voltage | 800 V |

30 nM solution of reconstitutable apoprotein was prepared in 1.5 ml quartz cuvette with magnetic stirrer and KPP buffer as blank for zero value plus 3 more cuvettes for triplicate

measurements on fluorimeter under the settings given in Table 9. First only buffer was measured as overall zero point, then apoprotein was added and measured with setup for Trp signal. Finally, FAD was titrated according to the pipetting protocol given in Table 10.

**Table 10.** Pipetting protocol for determination of reconstitutable apoprotein

| Steps | Volume (µl) | Final FAD concentration (µM) | Stock FAD concentration (µM) |
|---|---|---|---|
| 1 | 15 | 0.025 | 2.5 |
| 2 | 15 | 0.050 | 2.5 |
| 3 | 15 | 0.100 | 5.0 |
| 4 | 15 | 0.200 | 10.0 |
| 5 | 15 | 0.400 | 20.0 |
| 6 | 15 | 0.800 | 40.0 |
| 7 | 15 | 1.600 | 80.0 |
| 8 | 15 | 3.200 | 160.0 |

*3.3.3.4. Setup for FAD signal fluorescence of MtDH_N700G_N748G*

The measurements for *MtDH_N700G_N748G* were conducted under the fluorimeter settings given in table 11 and according to the pipetting protocol given in table 12.

**Table 11.** Fluorimeter settings for FAD signal

| | |
|---|---|
| Excitation | 450 nm |
| Emission | 485-1000 nm |
| Excitation Slit | 10 nm |
| Emission Slit | 20 nm |
| Voltage | 650 V |
| Speed | 2400 nm/min |
| Average time | 0.05 s |
| Interval | 2 nm |

100 nM solution of reconstitutable apoprotein was prepared in 1.5 ml quartz cuvette with magnetic stirrer and KPP buffer as blank in triplicate for zero value plus 3 more cuvettes for triplicate measurements under fluorimeter settings from Table 11. First only buffer was measured as overall zero point, then apoprotein was added and measured, finally FAD was titrated by pipetting protocol given in Table 12.

**Table 12.** Pipetting protocol for determination of reconstitutable *Mt*DH_N700G_N748G apoprotein

| **Steps** | **Volume (µl)** | **Final FAD concentration (µM)** | **Stock FAD concentration (µM)** |
|---|---|---|---|
| 1 | 7.5 | 0.0125 | 2.5 |
| 2 | 7.5 | 0.025 | 2.5 |
| 3 | 7.5 | 0.0375 | 2.5 |
| 4 | 7.5 | 0.050 | 2.5 |
| 5 | 7.5 | 0.075 | 5.0 |
| 6 | 7.5 | 0.100 | 5.0 |
| 7 | 7.5 | 0.150 | 10.0 |
| 8 | 7.5 | 0.200 | 10.0 |
| 9 | 7.5 | 0.300 | 20.0 |
| 10 | 7.5 | 0.500 | 40.0 |
| 11 | 7.5 | 0.700 | 40.0 |
| 12 | 7.5 | 1.100 | 80.0 |
| 13 | 7.5 | 1.500 | 80.0 |

*3.3.3.5. Reflavination*

12 µL of 100 nM reconstitutable apoprotein are mixed with 12 µL FAD (saturating amount; ~10x $K_D$) and activity is detected after 1h incubation. The $K_D$ measurement was performed by measuring 8 different FAD conc. (0 - ~10x $K_D$), together with blanks (without apoprotein).

*3.4.3.6. FAD loading of GMCs*

Since FAD bound in a protein complex doesn't necessarily follow the behavior of free FAD in a solution, molar absorbance can be different and also the peak maximum can be different, therefore leading to the difference in molar absorption coefficient. To calculate exact concentration of active enzyme and with specific activity, we needed to calculate the real molar absorbance coefficient for every enzyme studied. For that purpose we needed to separate FAD from the protein by denaturation with trichlor acetic acid (TCA). 450 µL solution of 20 µM holoprotein (protein loaded with FAD) was prepared and separated into volumes of 220 µL in 2 Eppis. For the enzymes that weren't fully loaded with FAD, higher concentration was necessary to have at least 10 µM final FAD concentration, so the absorbance can be accurately detected. As a blank we used 220 µL buffer in a 3$^{rd}$ Eppi. 10 µL 100% TCA was added to the Eppis to destroy the holoprotein and to buffer. For the holoprotein spectra, 10 µL buffer was added instead of TCA. TCA treated holoprotein sample was centrifuged at 15000 rpm to pellet the denatured protein. The solutions were then neutralized with 9 µL 5 M NaOH.

UV/VIS Spectra was recorded using a 1 cm, 200 µL quartz cuvette. Buffer was used as blank for the holoprotein and TCA treated buffer as blank for the supernatant from the denatured holoprotein to detect free FAD only. Accurate molar absorption factors were calculated for protein bound FAD based on the difference between the peak heights in UV/VIS spectra at 280 nm recorded using Diode Array spectrophotometer.

## 3.4. PROTEIN QUALIFICATION AND CHARACTERIZATION

### 3.4.1. SDS-PAGE electrophoresis

For the separation and qualification of chimeric product and its components and to determine efficiency of purification steps, precast SDS Mini-Protean TGX precast gels (Bio-Rad Laboratories, California, USA) with 4-20 % gradient. Protein solutions were mixed in 1:1 ratio with Laemmli-Buffer (Thermo Fisher Scientific, Waltham, Massachusetts, USA), denatured on thermo block for 15 minutes at 99 °C and analyzed using a Gel Doc XR and Image Lab software (Bio-Rad, USA). Seeblue Prestained Standard (Invitrogen, Thermo Fisher, Waltham, Massachusetts, US) marker was used to determine the molecular mass.

### 3.4.2. Protein quantification

#### *3.4.2.1. Spectrophotometry*

Homogeneous enzyme concentration was determined in a 1 cm or 0.3 cm quartz cuvette, from the absorption at 280 nm, using the calculated molar extinction coefficient for each protein.

To convert between absorption and protein concentration Lambert-Beer law was used:

$$A = \varepsilon \cdot c \cdot l$$

A – absorption

ε – molar extinction coefficient [$M^{-1}$ $cm^{-1}$]

c – molar concentration [M]

l – pathlength [cm]

#### *3.4.2.2. UV-Vis spectrophotometry*

UV-Visible spectra of native, apo and reconstituted proteins were recorded from 200-900 nm at room temperature in aerobic conditions using Agilent 8453 UV-visible Spectroscopy System (Agilent Technologies, California, USA). The molar absorption coefficients at 280 nm for all proteins were calculated by using the mature amino acid sequence and the ProtParam program (http://web.expasy.org/protparam/). For the recombinant GMCs, molar absorption coefficients were calculated as was described. Cytochrome concentrations were measured according to absorption at 420 nm.

#### *3.4.2.3. Bradford Protein Assay*

Total protein concentration in crude extracts was determined by Bradford method invented by Bradford (1976). The reagent and the standards were purchased from Bio-Rad Laboratories (Hercules, California, US) and were prepared according to the manufacturer's instructions. Assay was carried out by mixing 15 µl of sample with 600 µl of Bradford reagents, left for incubation 15 minutes in the dark and measured against blank containing only the reagents. Measurements were performed using Beckman Coulter DU 800 spectrophotometer (Beckman Coulter, Brea, California, USA). Protein concentration was automatically calculated from the standard calibration curve for bovine serum albumin.

## 3.5. ENZYME ACTIVITY ASSAYS

### 3.5.1. DCIP assay

All solutions except the sample were pipetted according to the pipetting protocol given in Table 13, in a 1 mL microcuvette and incubated at 30 °C in a water bath for 20 minutes. Cuvettes were then placed in a cuvette holder and the reaction was started by addition of the enzyme. Decolorization was measured by detecting the absorption at 520 nm in a UV/VIS spectrophotometer (Lambda 35, Waltham, MA, US).
Cuvette with DCIP, Na-acetate buffer and glucose was used as a blank.

**Table 13.** Pipetting protocol for DCIP assay

| **Solution** | **Concentration** | **Volume** |
|---|---|---|
| DCIP solution (in 10% (v/v) ethanol) | 3 mM | 100 µl |
| Lactose solution | 300 mM | 100 µl |
| Na-acetate Buffer pH 4.0 | 100 mM | 780 µl |
| Enzyme solution | | 20 µl |
| Total volume in the cuvette | | 1000 µl |

### 3.5.2. ABTS assay

1 ml of total reaction volume in the cuvettes was measured by absorption at 420 nm by Lambda 35 UV/Vis spectrometer (Waltham, MA, US). The buffer is preheated to 30°C, and following the pipetting protocol in Table 14, the reaction starts by addition of enzyme after all other solutions are added.
ABTS standard assay was used to detect levels of $H_2O_2$ created by GOX after oxidation of glucose to gluconic acid while reducing its own FAD cofactor and a $O_2$ molecule to generate $H_2O_2$. ABTS reduces HRP and produces the green colored ABTS* radical. 2 mols of ABTS are needed for 1 HRP cycle, therefore to calculate activity of GOX the result (U $ml^{-1}$) has to be divided by 2.

**Table 14.** Pipetting protocol for ABTS assay

| **Solution** | **Concentration** | **Volume** |
|---|---|---|
| KPP buffer, pH 6.5 | 50 mM | 860 µl |
| D-Glucose | 1 M | 20 µl |
| ABTS | 10 mM | 50 µl |
| Horse Radish Peroxidase | 50 mM | 50 µl |
| Enzyme | | 20 µl |
| Total volume in the cuvette | | 1000 µl |

# 4. RESULTS AND DISCUSSION

The two parts of thesis and will be described with separately. The first part deals with the production of a chimeric enzyme for the purpose of creating a novel enzyme capable of direct electron transfer between the dehydrogenase domain and the cytochrome domain. Chimeric enzyme is created based on the model of already utilized enzyme in the third generation biosensors, which is cellobiose dehydrogenase (CDH), consisting of dehydrogenase domain connected via linker to the cytochrome domain. CDH is capable of interdomain electron transfer (IET) and the cytochrome domain of CDH transfers electrons to the electrode and is therefore capable of direct electron transfer to the electrode (DET). For the purpose of avoiding the unwanted mutations and for better monitoring of linker sequence, post translational conjugation via site-specific labeling of proteins facilitated by sortase A enzyme was used.

Since glucose dehydrogenase (GDH) has higher selectivity toward glucose (shares the selectivity with GOX), displays higher turnover numbers and has shown increased stability in comparison to CDH, therefore it is a desired dehydrogenase domain for chimeric enzyme. GDH used in chimeric enzyme was produced by other lab members in *P. pastoris X-33.*

Cytochrome c domain was recombinantly produced for the purpose of this experiment in *E. coli* NEB 5 alpha strain, with included LPETG motif which was recognized by sortase A enzyme.

Sortase A enzyme was recombinantly produced in in *E. coli* NEB 5 alpha strain and after purification it facilitated peptide bond between the GDH domain and the cytochrome *c* domain, therefore creating the chimeric enzyme.

The second part of this thesis aims to analyze and improve the stability of different flavoenzymes (*An*GOX native, *An*GOX*_pps*, *Gc*GDH*_pps* and *Mt*DH*_pps*) for the purpose of creating a more stabile enzyme for the use in third generation biosensors. GMC's cofactor (FAD) is the main factor of their stability, and it is not bound covalently. By introducing a covalent bond, it would be possible to increase stability, since it would be impossible for the FAD to dissociate from the active site of the enzyme. Enzymes were first deflavinated (their FAD cofactor removed) and then reflavinated with synthetic FAD. The reaction was monitored fluorimetrically and the results were graphically plotted to determine the dissociation constant. Values of these constants will give us greater insights into further enzyme engineering steps for third generation biosensors yielding greater stability.

## 4.1. CHIMERIC PROTEIN PRODUCTION

### 4.1.1. Sortase A production and purification

SortaseA gene, ligated with pET-21a vector with c-terminal His-tag sequence (relevant in purification) was transformed in two *E. coli* strains: BL21 and NEB-5 alpha. Transformation was confirmed by their growth on LB medium with Ampicillin as the selection marker. Both transformed strains were further cultivated in shaking flasks culture at 37 °C, until OD reached 0.4, then, the temperature was optimized for protein expression at 25 °C with an addition of IPTG for increased protein expression.

The rembinant sortase A cells were harvested and pelleted by centrifugation and washed from the LB media by rebuffering in Buffer A. Then they were lysed in the French press to release the sortase A from the cell. After removal of the cell debris by vacuum filtration, 80 ml of crude extract was loaded to 5 ml $Ni^{2+}$ HisTrap column (GE Healthcare, USA) under conditions given in Table 2. Immobilized $Ni^{2+}$ cations on HisTrap column selectively bounded histidine residues of histidine tag on produced sortase A protein. Fractions and the crude extracts were analysed on SDS electrophoresis and the results are shown in the Figure 7.

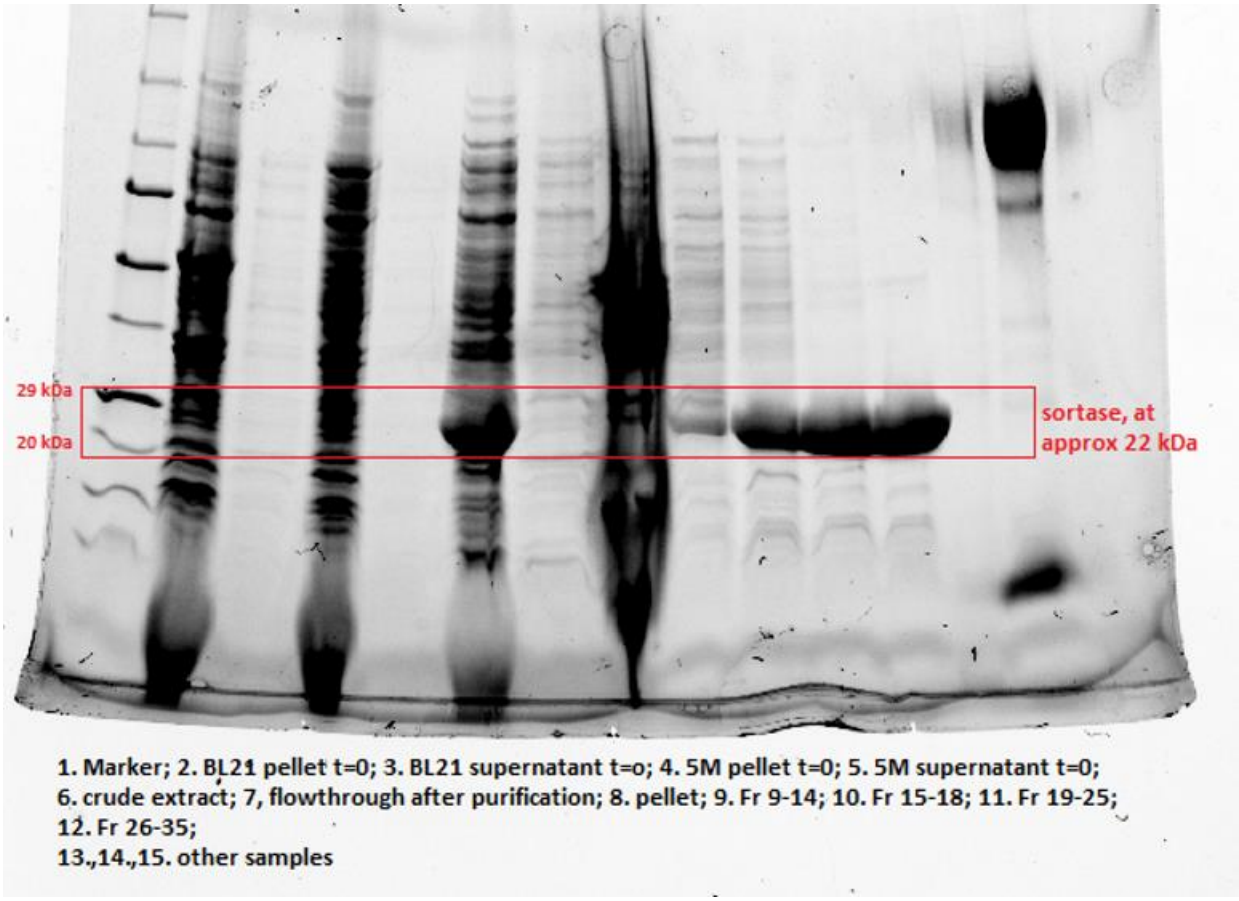


**Figure 7**. SDS page electrophoresis results, for both BL21 and NEB 5 alpha pentamutant *E. coli* production and purification of sortase A. Analyzed are all the fractions in purification steps: pellets, supernatants, crude extracts loaded to cromatography columns, purified sortase fractions, and the flowthrough after the cromatography. BL21 and 5M supernatant at t=0, was prepared by sonication at 30 pulses and then centrifugation at 15000 rpm for 5 min.

Molecular absorption coefficient calculated from the amino acid sequence was 17420 $\varepsilon_{450}$ [$M^{-1}$ $cm^{-1}$].

Molecular weight was 21677,36 Da, calculated based on aminoacid sequence by https://web.expasy.org/protparam/ webpage.

Total protein concentration in crude extract of NEB-5 alpha pentamutant (5m) cells, measured by absorption at 280 nm was 25.24 mg/ml * 80 ml (total volume of crude extract), giving the total quantity of protein of 2019.2 mg, and the amount of sortase was finally 7 % of all the protein that was present in the crude extract.

Total protein concentration in crude extract of BL21 cells, measured by absorption at 280 nm was 17.311 mg/ml * 102 ml (total volume of crude extract), giving the total quantity of protein protein of 1747.26 mg, and the amount of sortase was finally 5% of all the protein.
For further sortagging reaction, sortase from *E. coli* NEB 5 alpha pentamutant cells were used since the yield was higher.
Protein concentration in fractions was measured photometrically with diode meter, and acquired protein concentrations are given in the Table 15.

**Table 15.** Sortase A concetrations in fractions after $Ni^{2+}$ Histrap cromatography, measured with Bradford assay

| **Fraction** | **Absorption at 280 nm (dilution 1:3)** | **mg/ml** | **Total mg/ml** |
|---|---|---|---|
| FR 9-14 | 0.98131 | 1.2 | 12.2 |
| FR 15-18 | 0.69942 | 2.6 | 26.1 |
| FR 19-25 | 1.29760 | 4.8 | 48.4 |
| FR 26-35 | 1.41520 | 5.2 | 52.83203193 |
| | | | Σ= 139.6 mg |

4.1.2. Cytochrome *c* production and purification

pET-22b vector carryng N-terminal pelB sequence for potential periplasmic localization and C-terminal His-Tag sequence (needed for purification over $Ni^{2+}$ His trap column) was used for transformation of BL21 *E. coli* cells with gene for 3A9f cytochrome *c* with added LPETG motif. Successfullness of transformation was indicated by their growth on plates with LB medium and Campicillin as selection marker.
Scale-up of the production followed, by inoculating 3 L of fresh LB medium with Campicillin with 1 % v/v of the overnight culture, and incubation at 37 °C on a shaker. Growth of the culture was stopped when OD reached 0.4, and was placed at 25 °C with an addition of IPTG for protein expression.

Cells were harvested and pelleted by centrifugation and were then exposed to periplasmic shock induced by rebuffering in 20 % Tris Sucrose buffer at room temperature. After removal of the supernatant by centrifugation, periplasmic fraction containing the cytochrome was contained in the pellet. Pellet was further resuspended in 5 mm $MgSO_4$ an left for incubation for 15 minutes so the osmotic shock would be induced. Osmotic shock would relase the cytochromes from the periplasmic space into the supernatant. Color of the pellet was pink, and pink indicates the cytochrome presence, as shown on Figure 8. So the pellet was sonicated to lyse the cells and the rest of the cytochromes contained in the pellet was extracted to the liquid phase to improve yield.

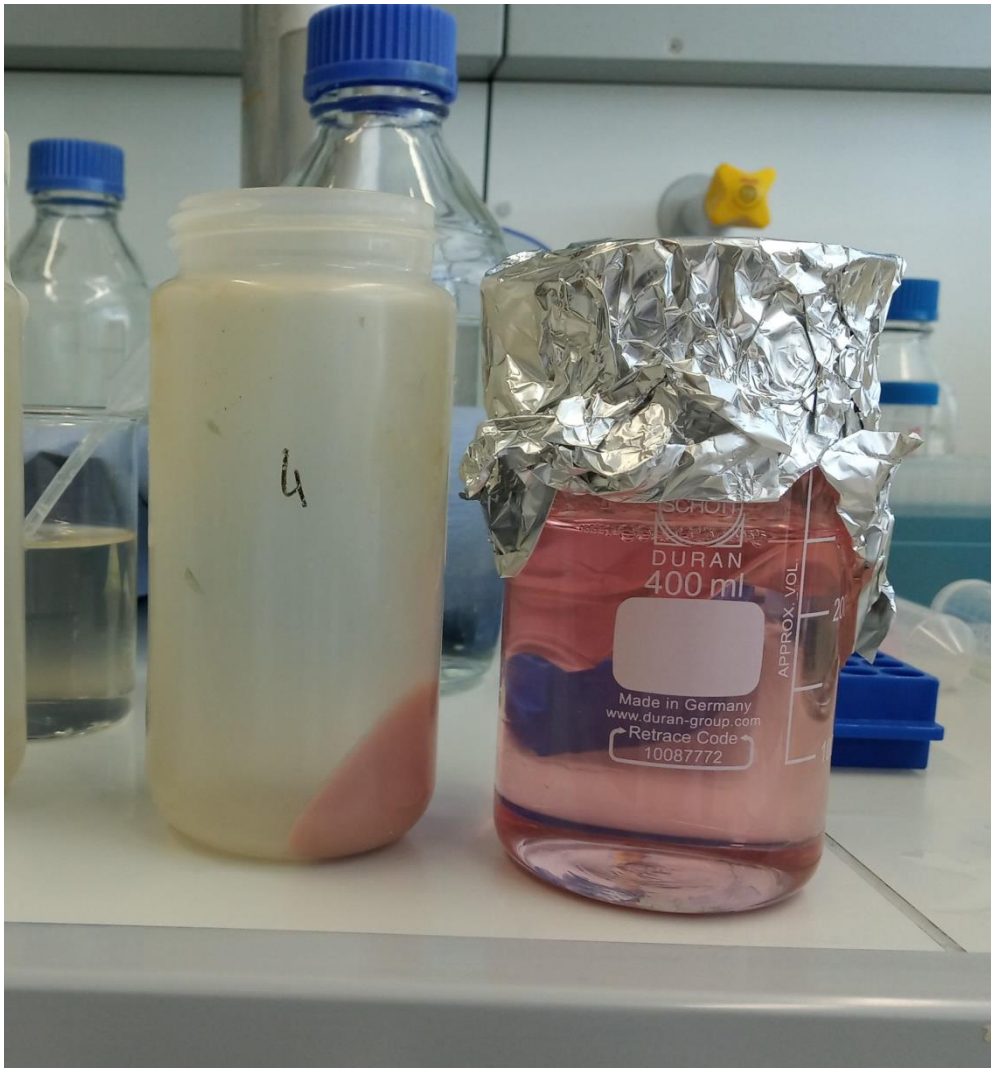


**Figure 8**. Pellet and supernatant containing cytochrome *c*

250 ml of crude extract (supernatant) containg the cytochromes was rebuffered in Buffer A, vacuum filtrated and loaded to 35 ml $Ni^{2+}$ HisTrap column with flow rate of 10 ml/min and fractioned using Äkta Explorer, $Ni^{2+}$ of the $Ni^{2+}$ HisTrap column bounded histidine residues on cytochromes and they were eluded with Buffer B in linear gradient. 1 ml protein fractions eluded were pooled together and intensively rebuffered in Sortagging buffer (50 mM Tris-HCl, 150 mM NaCl, 10 mM $CaCl_2$) pH 4.0 to reoxidize cytochromes and remove imidazole. Purification over $Ni^{2+}$ HisTrap column is shown on Figure 9 and the pink fractions on Figure 10.

**Figure 9**. Binding of the cytochromes on $Ni^{2+}$ His trap column

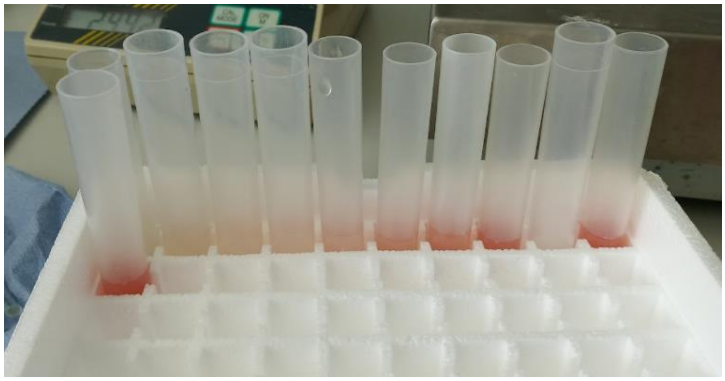

**Figure 10**. Eluded 1 ml cytochrome fractions, after purification on $Ni^{2+}$ His trap column

Pooled fractions were further loaded to Superdex 75 column to separate not fully matured apocytochromes (without heme cofactor) from cytochromes loaded with heme, and therefore active and needed for the sortagging assay.

4.1.3. Sortagging assay

Sortagging assay, e.g. mixing in the appropriate ratio of the of the GDH, cytochromes and the sortase in the same sortagging reaction, was carried out in the Amicon tubes with the cutoff at 30 kDa. Cytochromes and the GDH were mixed in a ratio 5:1 and the sortase wass added in the ratio 1:10 compared to the GDH. The reaction mix was incubated for 3 h at 30 °C in 20 ml Amicon tube. During the incubation period sortase A recognized LPETG motif on cytochromes, cleaving the motif between T and G, and formed the peptide bond with the G tags on GDH, thus creating cytochrome *c*-LPET-G-GDH chimeric product. Assay was performed in a centrifuge so the G-tags (glycins) pass to the supernatant and the LPETG motif on cytochrome *c* wouldn't again be connected to the G-tags, already cleaved by the sortase A. Sortase A with the molecular weight of around 22 kDa was also removed by centrifugation and contained in the flowthrough.

4.1.4. Purification of the chimeric enzyme

Sortagging mix, containing chimeric enzyme, unreacted GDH and unreacted cytochromes was further purified by connecting the $Ni^{2+}$ His Trap column and the Mono S ™ column on Äkta Pure system. The combined system of cromatography columns was used to bind the chimeric enzyme with the His tags. Unreacted GDH and the unreacted cytochromes were separated from

the chimeric protein and the efficiency of the purification was qualified over SDS page electrophoresis. The results of the purification of the sortagging mix are shown on Figure 11.

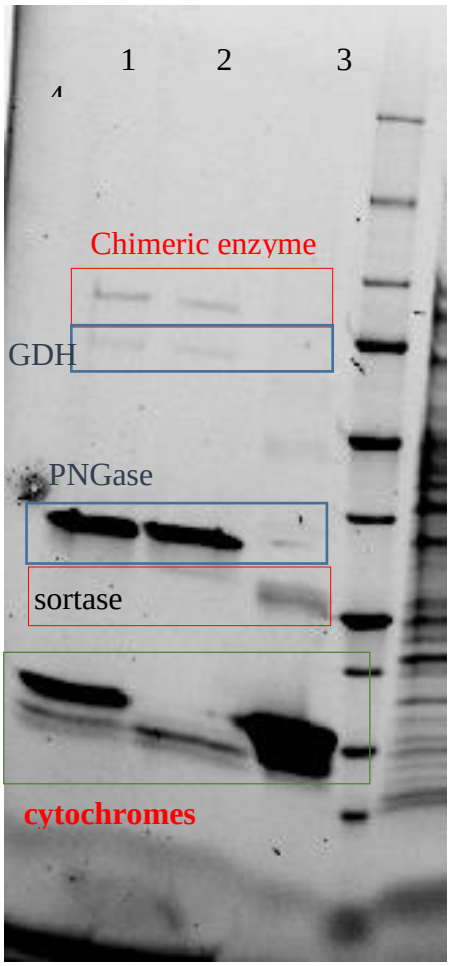


**Figure 11.** Results of the SDS page electrophoresis of the sortagging reaction mix in the 1st well; HisTrap flowthrough (2nd well) ; HisTrap eluate (3rd well) and a marker (4th well)

Cytochromes occur at 12 kDa, and are especially present in the His Trap eluate, at 22 kDa sortase occurs, and at around 66 kDa the chimeric enzyme. GDH was deglycosylated with PNGase enzyme (New England Biolabs) because if glycosylated, it would be too big for qualification on SDS gel.

There are some residual GDH molecules, because the MonoS column wasn't very good.

The reaction and purification were successful, but with low yield of chimeric product, around 300 µL with the concentration of 34 µM, with efficiency compared to GDH concentration of more than 50 %. Product was confirmed by mass spectrometry and was further tested for DET

by cyclic voltammetry by supervisor. DET was possible, but the diffusion of glucose through the dialysis membrane immobilizing the enzyme on the electrode was very slow, and further optimization of the electrochemical measurements was needed.

## 4.2. $K_D$ DETERMINATION

### 4.2.1.Deflavination

Some tested enzymes needed more cycles, and some couldn't even be precipitated as is shown in the Table 16. A possible reason for this phenomenon could be different glycosylation pattern of the different proteins.

**Table 16.** Enzymes tested for deflavination

| **Enzyme studied** | **Precipitation** | **Cycles** |
|---|---|---|
| Native *An*GOx (Sigma Aldrich) | yes | 1-2 |
| *An*GOx_pps (*P. pastoris* Superman5) | yes | 2 |
| *Gc*GDH | yes | 2 |
| *Mt*DH N700S/N748 Oxy+ | yes | 5-7 |
| *An*GOx_pps (*P. pastoris* X33) | no | |
| *Mt*DH from wild type X33 | no | |

*Pichia pastoris* usually expresses high levels of highly-glycosilyted recombinant proteins, so due to the excessive glycosylation, the solubility of the proteins must be higher, hence this fact lead to the problem that no or less protein could be precipitated by saturated ammonium sulfate solution (salting out procedure), which decrases the yield of apoenzyme.

*Mt*DH_N700S/N748G had to be precipitated multiple times because of the higher initial FAD loading (which will be explained later in FAD loading) and due to the asparagins at 700 and 748$^{th}$ place covering the cofactor pocket.

*P. pastoris* Superman5 strain was transformed using a GlycoSwitch vector, introduction of which is necessary for the conversion of any wild-type *Pichia* strain into a strain that modifies it's glycoproteins with Gal2GlcNAc2Man3GlcNAc2 *N*-glycans. This is a strategy to convert *Pichia*

*pastoris* heterogeneous high mannose-type *N*-glycosylation to more mammalian-like hybrid and complex *N*-glycans, (Jacobs et al., 2009; Laukens et al., 2015) they are less soluble, therefore precipitation and characterization was possible. This can be of pivotal importance to generate the appropriate glycoforms of therapeutically relevant glycoproteins or to gain a better understanding of structure–function relationship (Laukens et al., 2015).

First step of the Swoboda et al. deflavination protocol (mixing 50 µl of 15-30 mg $ml^{-1}$ of enzyme solution with 50 µl 50 mM KBr) resulted in a satisfactory apoprotein yield only in native *An*GOX case. The starting concentrations of recombinant enzymes were higher in order to produce enough apoproteins for further analysis.

### 4.2.2. Fluorescence measurements

Successfully deflavinated and precipitated apoproteins suspended in KPP buffer were kept on ice in the fridge until further analysis. After every thawing some of the apoprotein would precipitate and the precipitate would be discarded, since it has denaturized and therefore couldn't be active even if reflavinated. Supernatant was vortexed and the new concentration was measured every time on Diode Array to obtain best possible measurement results. Every week new apoproteins were produced as the method developed.

Finally the experiment was designed in a way that the free and bound FAD was measured based on the tryptophan (Trp) signal of tryptophan residues close to the binding site of FAD. Binding of FAD changes the conformation of the binding site and subsequently changes the fluorescence signal, and from the difference in peak heights it was possible to calculate the $K_D$ value given the concentrations of stock FAD and apoprotein were correctly calculated.

Trp signal was excited at 280 nm and the emission was visible between 300 and 400 nm, with Peak maximum ~340 nm for every enzyme analyzed.

Signal of the free FAD can be excited at 280, 380 and 450 nm, and the emission is visible between 500 and 550 nm, with Peak maximum at ~525 nm.

### 4.2.3. $K_D$ values

$K_D$ values for each enzyme were calculated by plotting the free and bound FAD fluorescence signal at 525 nm within a nonlinear minimal squares regression model based on the Michaelis

Menten equation, applying SigmaPlot 12.5 with enzyme kinetics add-on (Systat Software, San Jose, California, USA) and by https://mycurvefit.com/, plotting website with Michaelis Menten function. Furthermore, the results were confirmed by transformation of acquired data to linear form and plotting it according to Scatchard equation. Fractional saturation Y of apoprotein molecules (enzyme) saturated with ligand (FAD) (with the assumption of 1:1 stoichometry - one mole of ligand per one mole of enzyme) was plotted as a function of bound FAD concentration and the result was a straight line with a slope of $-1/K_D$ and the intercept of the binding function with the Y-axis gives $1/K_D$ value. Using the hyperbolic binding curve for plotting the FAD bound vs. FAD free, we can graphically get to the value of constant of dissociation $K_D$. The plotted results for *An*GOX_nat are shown in Figures 12 and 13; for *An*GOX_pps in Figures 14 and 15; for *Gc*GDH_pps in Figures 16 and 17 and for *Mt*DH_pps in Figures 18 and 19. $K_D$ values of enzymes studied, acquired by fluorescence measurements are summed up with the $K_D$ values from the activity assays in the Table 18.

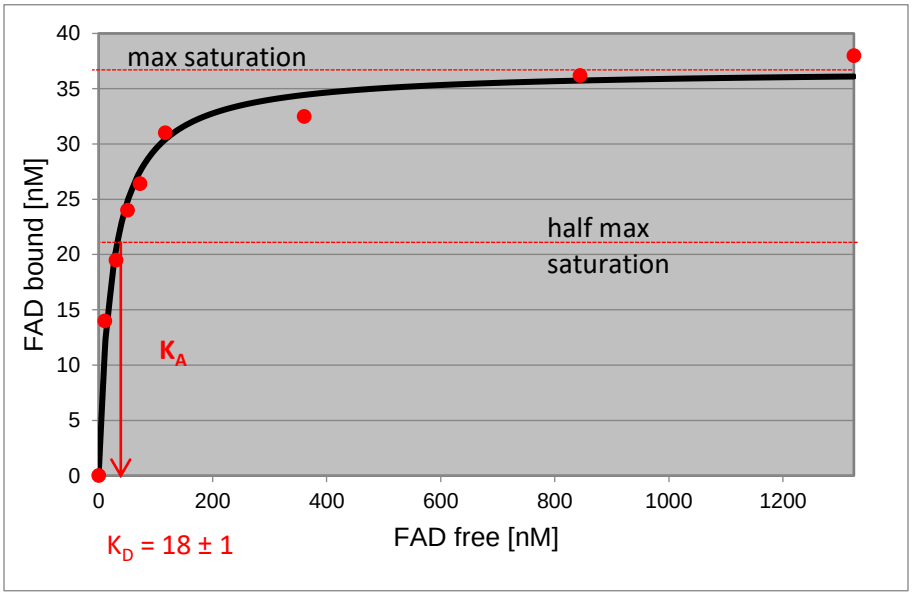


**Figure 12**. Hyperbolic binding curve for *An*GOX_nat at 340 nm, $K_D = 18 \pm 1$ nM

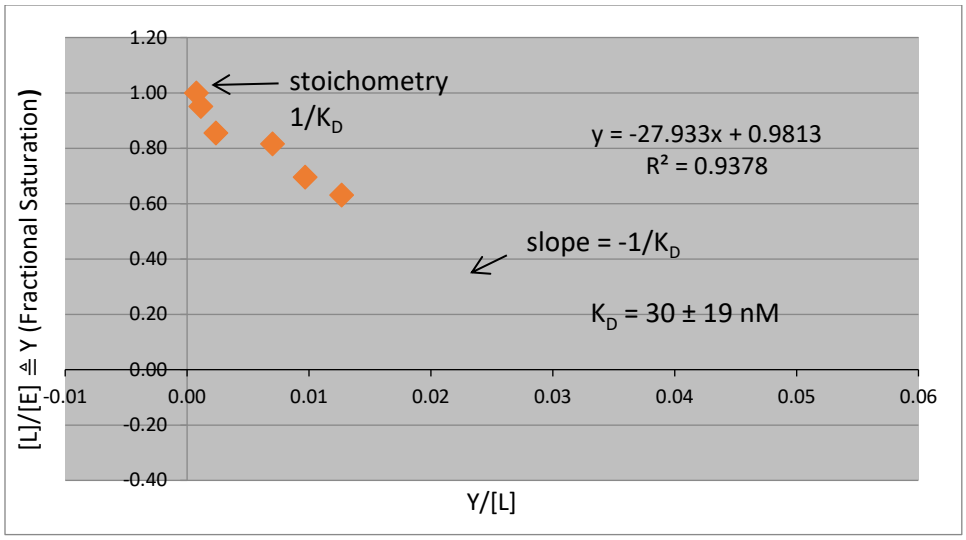


**Figure 13**. Scatchard plot for *An*GOX_nat at 340 nm

$K_D$ value for *An*GOX_nat was calculated based on the intercept of the binding function with the x and y axis, which was 0.986/0.033 and it equals 30 ± 19 nM.

The same principle was used for *An*GOX_pps and *Mt*DH_pps:

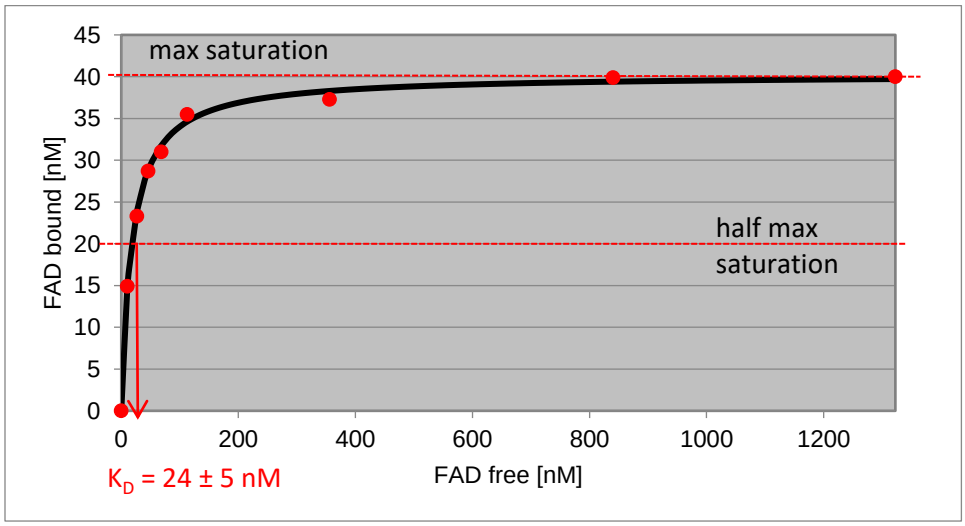


**Figure 14**. Hyperbolic binding curve for *An*GOX_pps at 340 nm, $K_D$ = 24 ± 5 nM

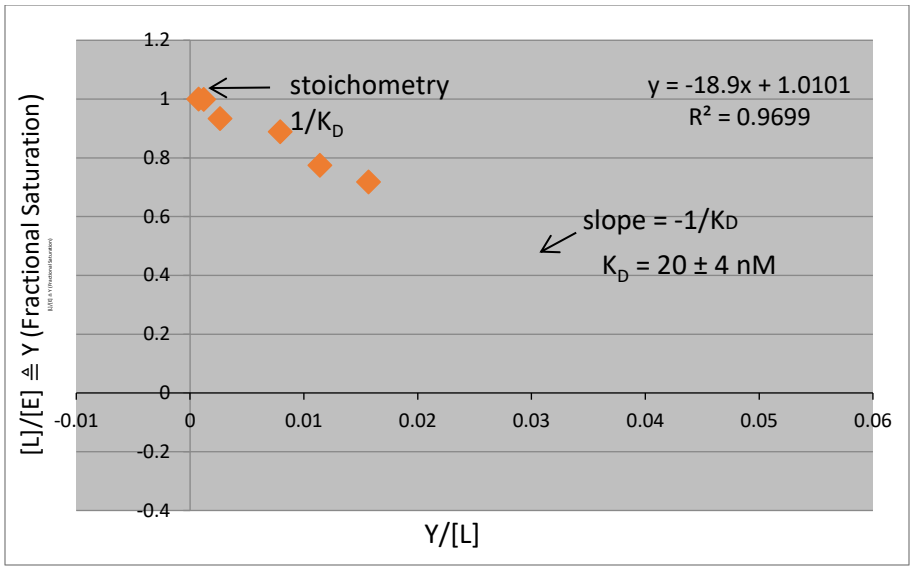


**Figure 15.** Scatchard plot for *An*GOX_pps at 340 nm

$K_D$ value for *An*GOX_pps was calculated based on the intercept of the binding function with the x and the y axis, which was 1.009/0.051 giving the value of 20 ± 4 nM.

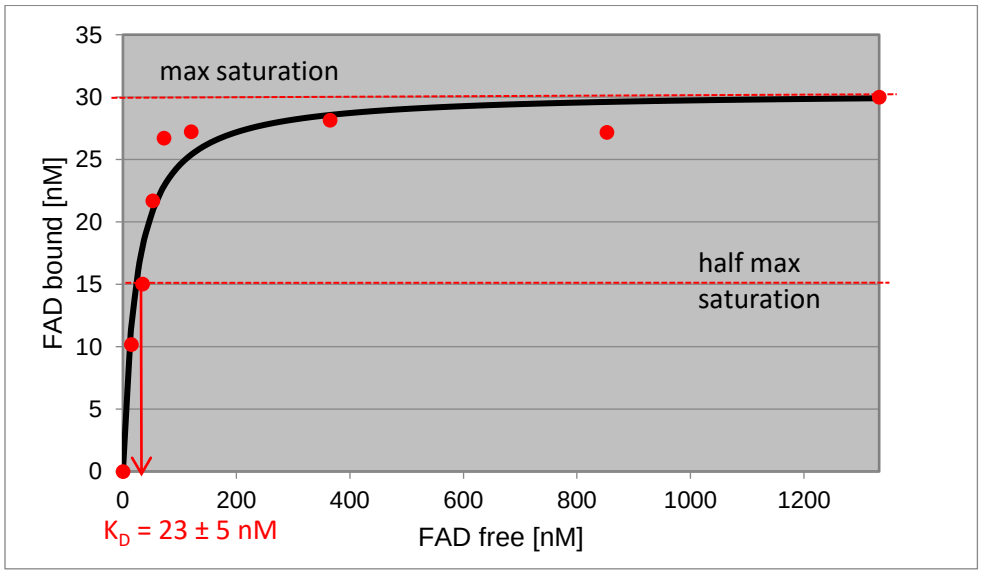


**Figure 16.** Hyperbolic binding curve for *Gc*GDH at 340 nm, $K_D$ = 23 ± 5 nM

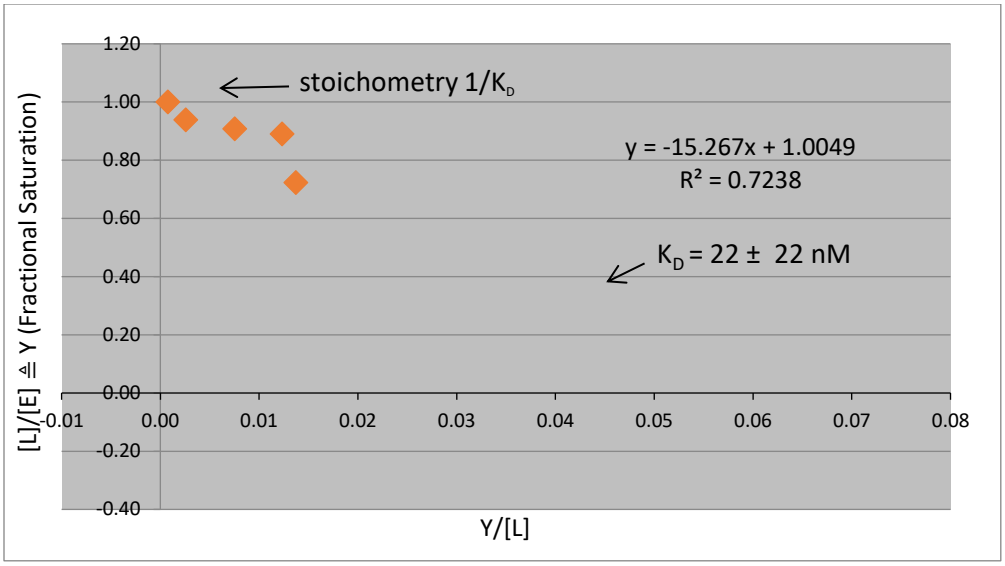


**Figure 17.** Scatchard plot for *Gc*GDH at 340 nm

$K_D$ value for GDH was calculated based on the intercept of the binding function with the x and y axis, which was 0.999/0.045 giving the value of 22 ± 22 nM.

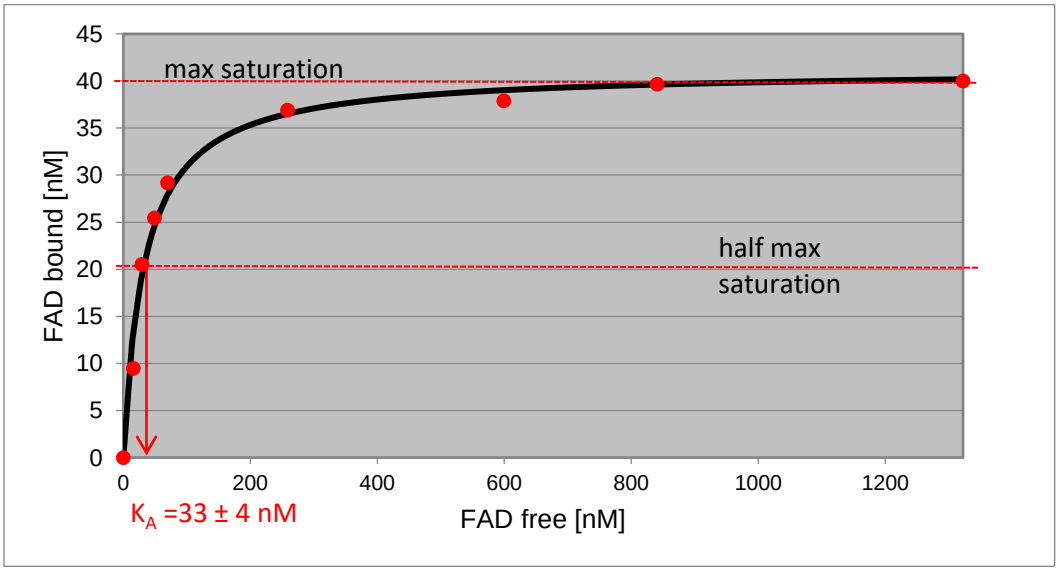


**Figure 18.** Hyperbolic binding curve for *Mt*DH_pps at 340 nm, $K_D$ = 33 ± 4 nM

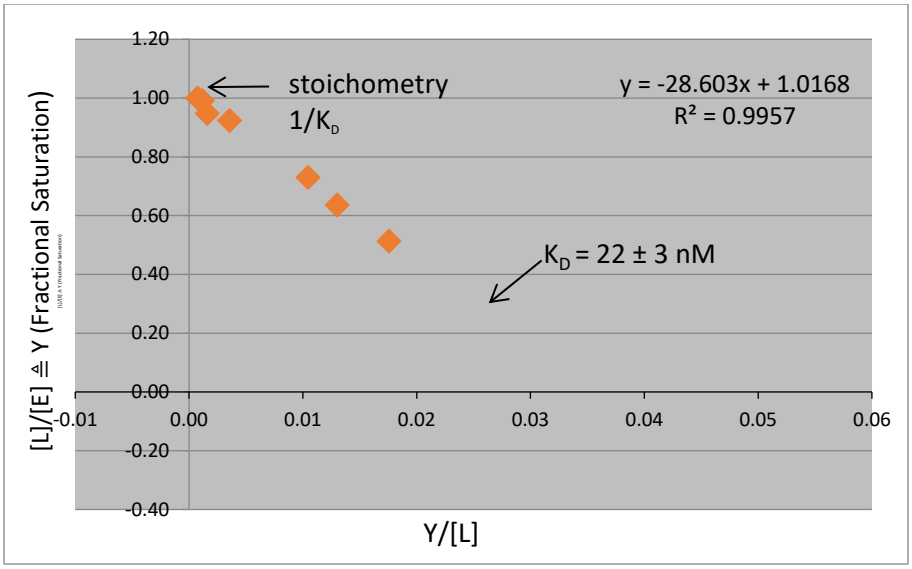


**Figure 19**. Scatchard plot for *Mt*DH_pps at 340 nM

$K_D$ value for *Mt*DH was calculated based on the intercept of the binding function with the x and y axis, which was 1.017/0.035 giving the value of 22 ± 3 nM.

4.2.4. FAD loading of holoproteins

Quantification of flavoenzyme solutions with UV/VIS spectrophotometry was mainly based on the FAD absorption spectra at 450 nm and calculated with the extinction coefficient of FAD $\varepsilon_{450}$ = 11 300 $M^{-1}$ $cm^{-1}$, but following the realization that not all apoprotein is reconstitutable, the possibility that not all holoproteins were FAD loaded and therefore active had to be examined.

Protocol for FAD loading determination with TCA was described in 3.4.3.6. It is a procedure established by Swoboda in 1964. After denaturizing the proteins with acid and high temperatures, FAD was liberated from the cofactor site and absorption of free FAD was measured against the buffer treated with TCA for zero value. Concentration of denaturized protein was measured on a Diode Array in UV/VIS spectra, by absorption at 280 nm (with an exception of full CDH with cytochrome) against the buffer for zero value. An example of a recombinant *An*GDH_pps sample is shown in Figure 20.

Absorption of the recombinant, as well as the native *An*GOX is lower than that of the free FAD, and *An*GOX_nat and *Gc*GDH_pps's peak maximum has shifted from 450 to 453 nm (GOX) and 460 nm (GDH). Only the *Mt*DH absorption stays the same, possibly because of the loop motif

covering the FAD being shorter than in the other enzymes analyzed, without anything changing the fluorescence significantly. New molecular absorption coefficients (**$\varepsilon_{450}$**) specific to each enzyme had to be recalculated, based on the molecular absorption coefficient of the free FAD. New values are shown in Table 17 and will help in more accurate quantification and subsequently characterization of enzymes.

**Table 17**. New extinction coefficients of analyzed enzymes

| **Enzyme** | **Molecular absorption coefficient $\varepsilon_{450}$ [$M^{-1}$ $cm^{-1}$]** |
|---|---|
| *An*GOX_nat | 14182 |
| *An*GOX_pps | 14286 |
| *Gc*GDH | 12383 |
| *Mt*DH_N700_N748 | Stays the same |

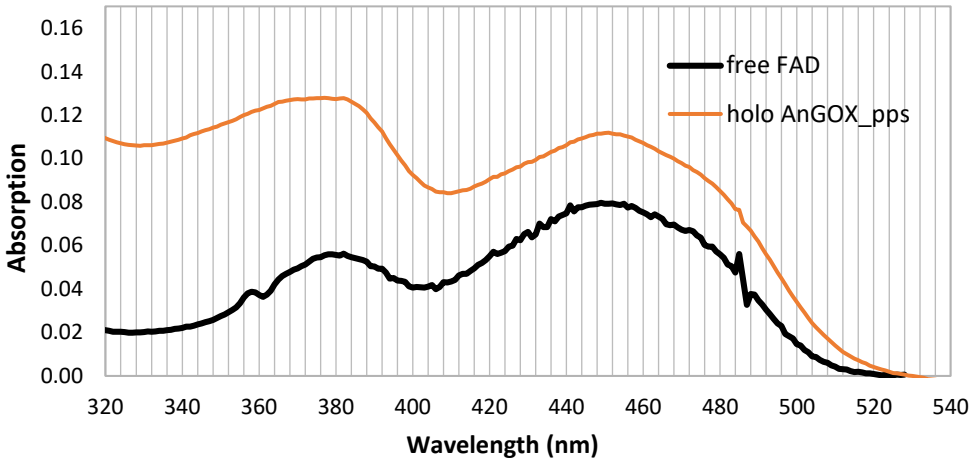


**Figure 20**. Absorption spectra of the holo*An*GOX_pps and free FAD extracted from *An*GOX_pps

### 4.2.5. $K_D$ determination by activity assays

Apoproteins were reflavinated by mixing with the saturating amount (~10x $K_D$ of stock FAD) and activity was detected after 1h of incubation. The measurements were conducted with 8 different FAD concentrations (0- ~10x $K_D$), together with blanks containing only FAD and buffer.

Concentrations of reconstitutable apoproteins were determined based on holoprotein activities. After the reflavination incubation period, enzyme solutions were prepared so the volumetric activities (not divided by 2) would be around 33 U $ml^{-1}$. In an ideal case, spectrophotometer would measure the absorption change of (de)colored enzyme reactions and absorption values would fit in the device's range of detection (0.15- ~0.9 Abs), so the dilutions of reconstitutable apoproteins were prepared accordingly. Two out of four enzymes studied in this thesis were analyzed in this way and the resulting $K_D$ values can be seen in the Table 18, together with the $K_D$ values measured with fluorimeter.

#### *4.2.5.1. ABTS activity assay of native AnGOX*

ABTS activity assay was conducted according to the standard procedure described in 3.6.2., only the concentration was optimized to fit the detection span of spectrophotometer.

60 nM apo*An*GOX was prepared from 13.70 µM stock and was mixed 1:2 with with FAD. Concentration of reconstitutable apo*An*GOX was calculated based on holo*An*GOX volumetric activity of 2650 U $ml^{-1}$. Apo*An*GOX was mixed with stock FAD of preestablished concentrations (0; 12.5; 37.5; 75; 150; 300; 600; 1200) µM. Residual activity of apo*An*GOX was substracted from mean value of activities for every FAD titration measured in triplicates. From the values for volumetric activity of enzyme reflavinated with different, known, concentrations of FAD, values for free and bound FAD were obtained and plotted to the hyperbolic binding curve (Figures 21 and 23) and Scatchard plot in Figure 22.

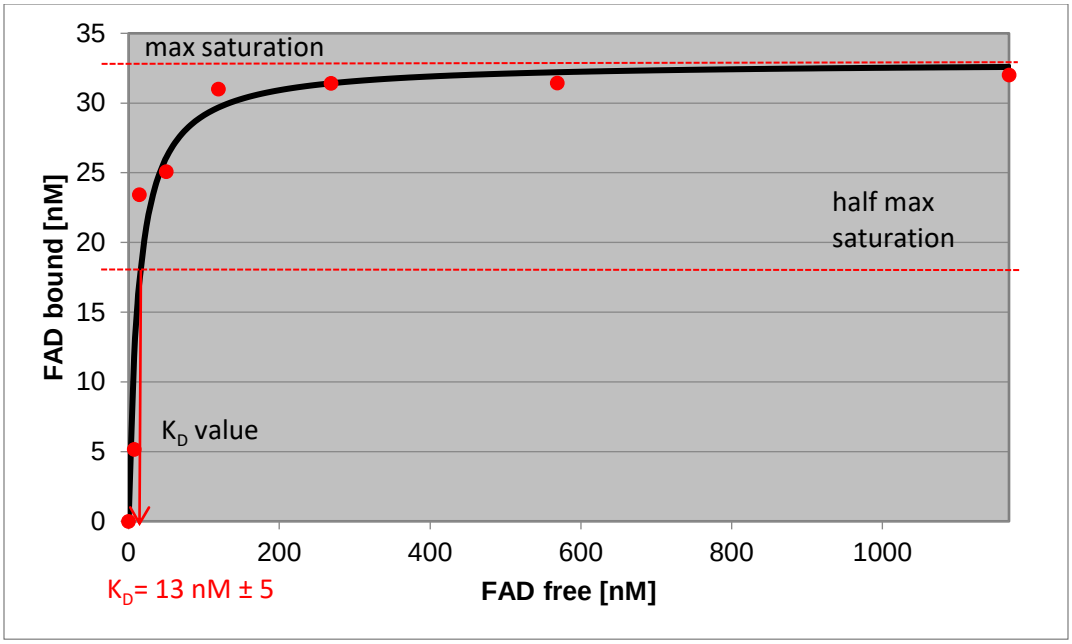


**Figure 21**. Hyperbolic binding curve representing the FADs affinity ($K_D$ value) for apo*An*GOX acquired by ABTS activity measurement

$K_D$ value was calculated by https://mycurvefit.com/, plotting website with Michaelis Menten function.

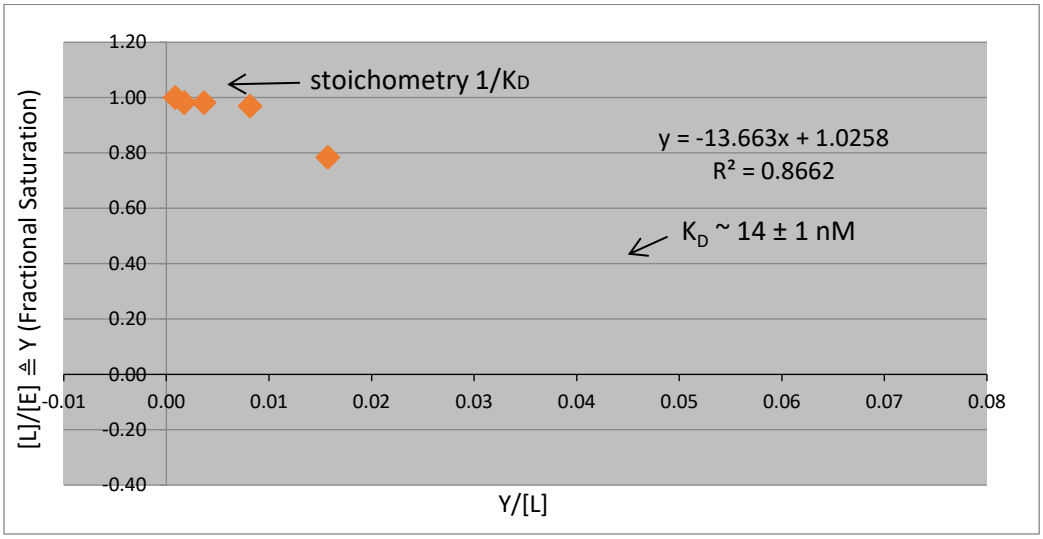


**Figure 22.** Scatchard plot for *An*GOX_native based on the ABTS activity

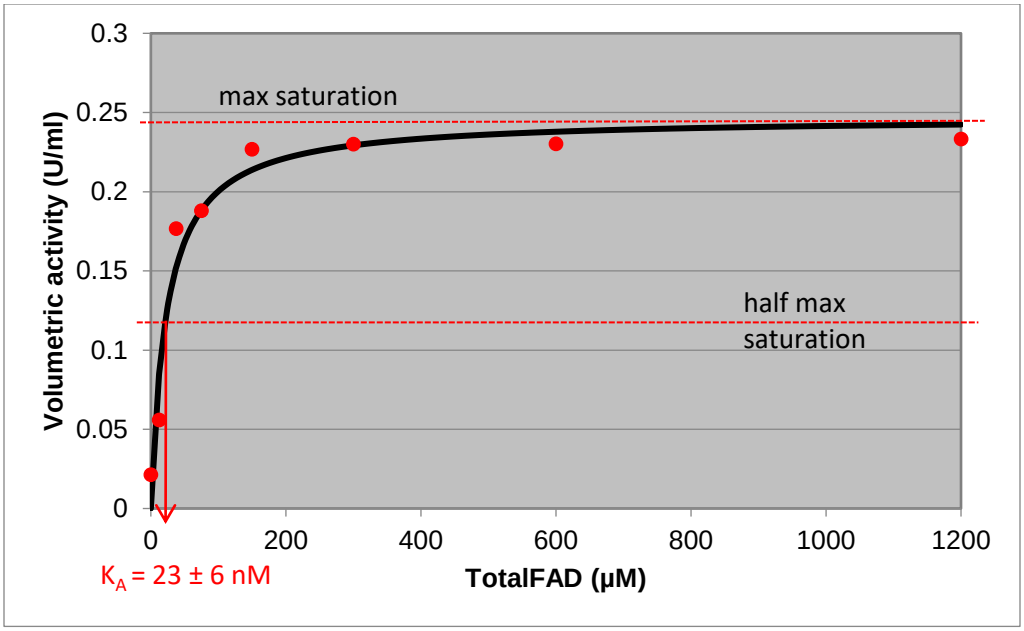


**Figure 23**. Hyperbolic binding curve representing the FADs affinity ($K_D$ value) for apo*An*GOX acquired by ABTS activity measurement $K_D$ = 23 ± 6 nM

*4.2.5.2. DCIP activity assay of Mt*DH_N700S/N748G

DCIP activity assay was conducted according to the standard procedure described in 3.6.3., only the concentration was optimized to fit the detection span of spectrophotometer. Volumetric activity measurements were carried out at 520 nm, with

60 nM apo*An*GOX was prepared from 13.70 µM stock and was mixed 1:2 with with FAD. Concentration of reconstitutable apo*An*GOX was calculated based on holo*An*GOX volumetric activity of 2650 U $ml^{-1}$. Apo*An*GOX was mixed with stock FAD of preestablished concentrations (0; 12,5; 37,5; 75; 150; 300; 600; 1200) µM. Residual activity of apo*An*GOX was substracted from mean value of activities for every FAD titration measured in triplicates. From the values for volumetric activity of enzyme reflavinated with different, known, concentrations of FAD, values for free and bound FAD were obtained and plotted to the hyperbolic binding curve (Figure 24 and 26) and Scatchard plot in Figure 25.

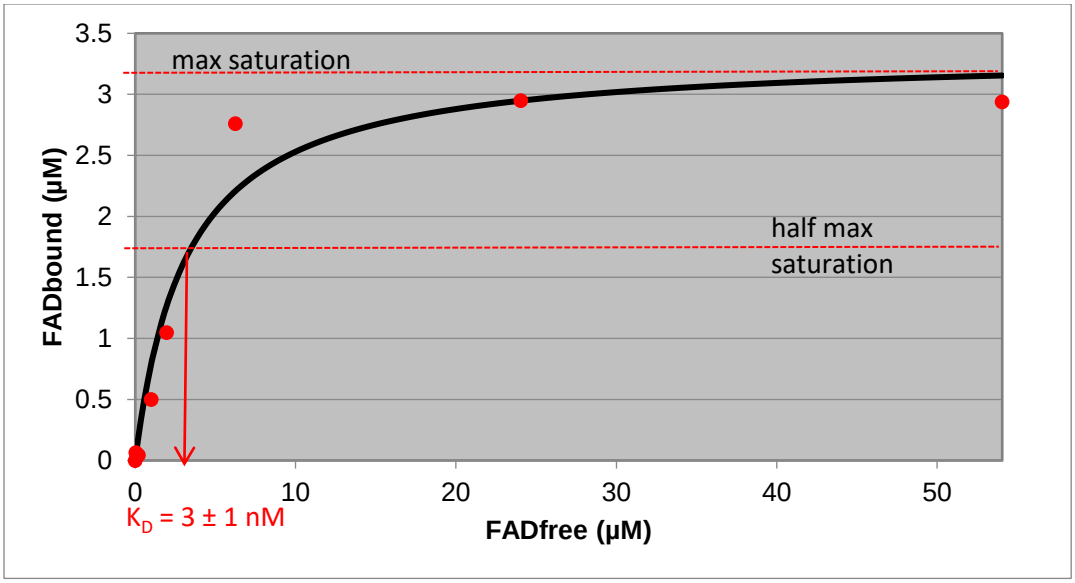


**Figure 24.** Hyperbolic binding curve representing the FADs affinity ($K_D$ value) for apo*Mt*DH acquired by DCIP activity assay $K_D$ = 3 ± 1.0 nM

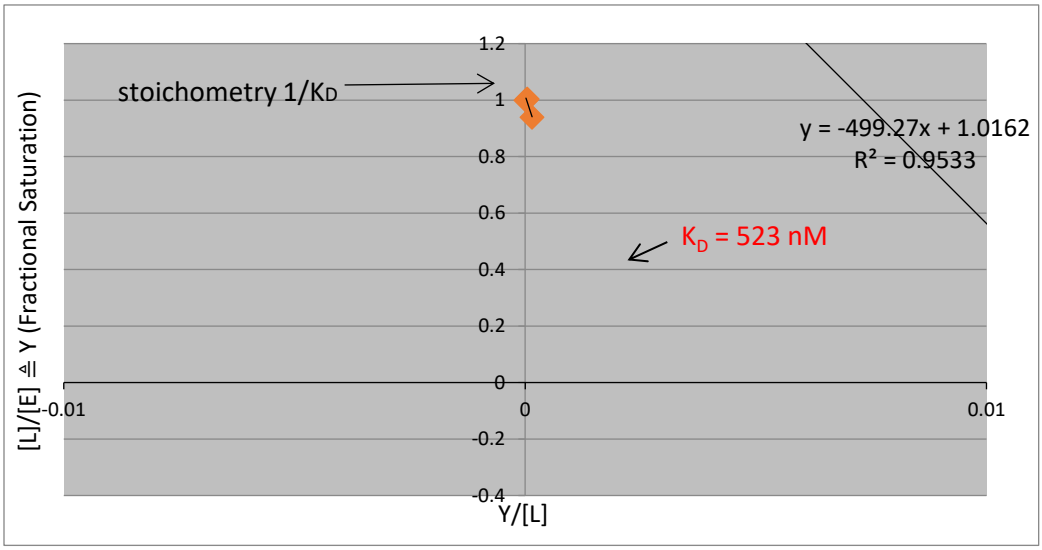


**Figure 25.** Scatchard plot for *Mt*DH based on the DCIP activity assay

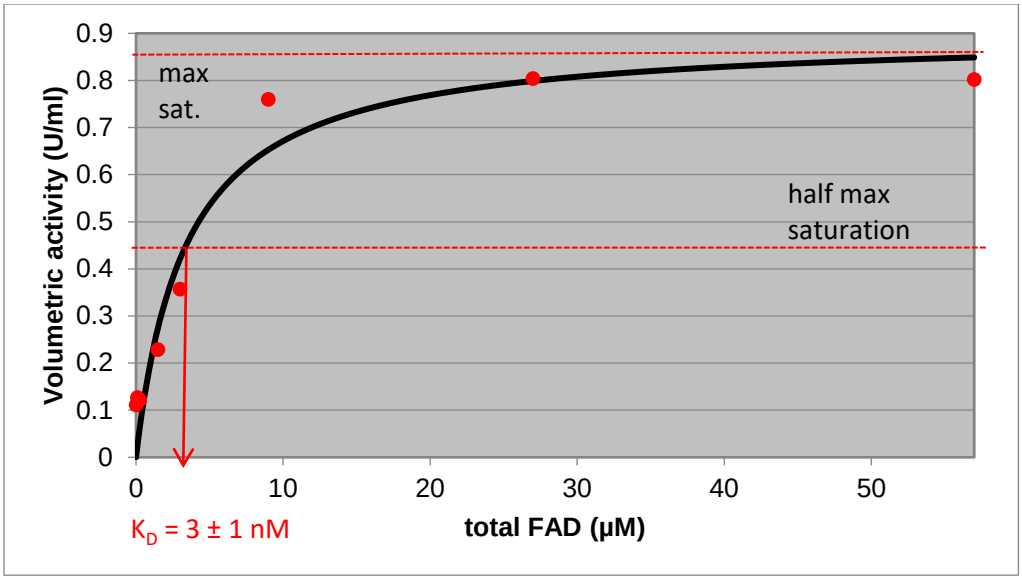


**Figure 26**. Hyperbolic binding curve representing the FADs affinity ($K_D$ value) for apo*Mt*DH acquired by DCIP activity assay

**Table 18**. $K_D$ values of enzymes studied

| **Enzyme analyzed** | **$K_D$ from hyperbolic curve fitting [nM]** | **$K_D$ from Scatchard plot [nM]** |
|---|---|---|
| *An*GOX_native 340 nm | 18 ± 1 | 30 ± 19 |
| *An*GOX_native 525 nm | 22 ± 2 | 29.73 |
| *An*GOX_native ABTS assay | 13 ± 5 | 14 ± 1 |
| *An*GOX_native ABTS activity assay | 23 ± 6 | n.d. |
| *Gc*GDH_*pps* 340 nm | 23 ± 5 | 22 ± 22 |
| *Gc*GDH_*pps* 525 nm | 33 ± 4 | |
| *Mt*DH_*pps* 340 nm | 33 ± 4 | 22 ± 3 |
| *Mt*DH_*pps* 525 nm | 21 ± 3.09 | 36 |
| *Mt*DH_*pps* DCIP assay | 3 ± 1 | 523 |
| *Mt*DH_*pps* DCIP activity assay | 3 ± 1 | n.d. |
| *An*_GOX_*pps* 340 nm | 24 ± 5 | 20 ± 4 |
| *An*_GOX_*pps* 525 nm | 47 ± 4 | 56 |

FAD binding affinity of all measured flavoenzymes are very similar. All $K_D$ values are in the low nanomolar range, which shows the high affinity of the cofactor FAD to the protein. Only *Mt*DH, which is lacking the cytochrome domain, shows a 10 times higher value. However, it is only if the DCIP is used for the measurement. Possible reason could be an artifact related to the assay or another relationship connected to the lack of cytochrome domain. Nevertheless, within this thesis there was not enough time to further investigate this relation, therefore we can only speculate about it.

The fact that the affinity is very high leads to the conclusion that the cofactor would be only hardly lost, which leads to another conclusion, which is that the reason for the inactivation of GMCs stems from another factors, such as the reaction of FAD with the reactive oxygen species, such as hydrogen peroxide, possible product in the GMC catalysis.

# 5. CONCLUSIONS

1. Chimeric protein was successfully produced in shaking flasks culture by sortase-mediated transpeptidation (sortagging), method for promotion of domain fusion in chimeric proteins by post-translational conjugation via site-specific labeling of proteins.

2. Chimeric GDH + cytochrome enzymes were previously expressed in *E. coli* strains, but their DET was inferior to the one of CDH. Post translational cojugation is the strategy for more effective and controlled linker design, crucial for obtaining adequate interdomain electron transfer (IET) and subsequently direct electron transfer to electrode (DET).

3. *Pichia pastoris* usually expresses high levels of highly-glycosilyted recombinant proteins, so due to the excessive glycosylation, the solubility of the proteins must be higher, hence this fact lead to the problem that no or less protein could be precipitated by saturated ammonium sulfate solution (salting out procedure), which decrases the yield of apoenzyme. Enzymes that couldn't be precipitated were *An*GOx_pps (*P. pastoris* X33) and *Mt*DH from *P. pastoris* wild type *X33.*

4. AnGOX_pps from *P. pastoris* Superman5 could be deflavinated and precipitated due to the GlycoSwitch vector technology

5. *Mt*DH N700S/N748G had to be precipitated multiple times because of the higher initial FAD loading and due to the asparagins at 700 and 748$^{th}$ place covering the cofactor pocket.

6. First step of the Swoboda et al. deflavination protocol (mixing 50 µl of 15-30 mg ml$^{-1}$ of enzyme solution with 50 µl 50 mM KBr) resulted in a satisfactory apoprotein yield only in native *An*GOX case. The starting concentrations of recombinant enzymes were higher in order to produce enough apoproteins for further analysis.

7. New molecular absorption coefficients at 450 nm **($\varepsilon_{450}$)** specific to each enzyme were recalculated, based on the molecular absorption coefficient of the free FAD. Each studied protein was denatured with TCA, and the absorption spectra of the apoprotein at 280 nm, and the liberated FAD at 450 nm was measured. Absorption of the recombinant, as well as the native *An*GOX is lower than that of the free FAD, and *An*GOX_nat and *Gc*GDH_pps's peak maximum has shifted from 450 to 453 nm (GOX) and 460 nm (GDH). New values will help in more accurate quantification and subsequently characterization of enzymes.

8. Not all apoprotein generated by deflavination can be reconstituted. By exciting the free FAD at 450 nm, and measuring the fluorescence emission spectra from 485 to 1000 nm and comparing it to the same concentration of FAD in an apoprotein solution, the concentration of

reconstitutable apoprotein can be calculated. Reconstitutable apoprotein concentration varies with each batch of prepared apoprotein, and the measurements have to be performed in a saturating amount (~10x $K_D$).

9. Knowledge of reconstitutable apoprotein concentration is necessary for accurate reflavinated enzyme activity measurements.

10. $K_D$ value of MtDH_N700S/N748G (Oxy +) acquired by DCIP activity measurement was much higher than that acquired by fluorescence measurement, but that is the case only if the DCIP is used for the measurement. Possible reason could be an artifact related to the assay or another relationship connected to the lack of cytochrome domain.

# 6. LITERATURE


1. Bhalla, N., Jolly, P., Formisano, N., Estrela, P. (2016) Introduction to biosensors. *Essays In Biochemistry* **60**, 1–8.

2. MarketsandMarkets™
   Biosensors Market with COVID-19 Impact by Type, Product (Wearable, Non-wearable), Technology, Application (POC, Home Diagnostics, Research Lab, Environmental Monitoring, Food & Beverages, Biodefense) and Region - Global Forecast to 2026 <https://www.marketsandmarkets.com/Market-Reports/biosensors-market-798.html> visited on September 30th 2021

3. Caldinelli, L., Iametti, S., Barbiroli, A., Fessas, D., Bonomi, F., Piubelli, L., Molla, G., Pollegioni, L. (2008) Relevance of the flavin binding to the stability and folding of engineered cholesterol oxidase containing noncovalently bound FAD. *Protein science: a publication of the Protein Society **17***, 409–419.

4. Cavener, D. R. (1992) GMC oxidoreductases. *Journal of Molecular Biology* **223**, 811–814.

5. Degani, Y., Heller, A. (1987) Direct electrical communication between chemically modified enzymes and metal electrodes. I. Electron transfer from glucose oxidase to metal electrodes via electron relays, bound covalently to the enzyme. *The Journal of Physical Chemistry* **91**, 1285–1289.

6. Garajová, K., Zimmermann, M., Petrenčáková, M., Dzurová, L., Nemergut, M., Škuléty, L., Žoldák, G., Sedlák, E. (2017) The molten-globule residual structure is critical for reflavination of glucose oxidase. *Biophys. Bio*. **230**, 74-83.

7. Hefti, M. H., Vervoort, J., Van Berkel, W. J. H. (2003) Deflavination and reconstitution of flavoproteins. *European Journal of Biochemistry* **270**, 4227–4242.

8. Jacobs, P. P., Geysens, S., Vervecken, W., Contreras, R., Callewaert, N. (2009) Engineering complex-type N-glycosylation in *Pichia pastoris* using GlycoSwitch technology. *Nature Protocols*, **4**, 58–70.

9. Juska, V.B., Pemble, M.E. (2020) A Critical Review of Electrochemical Glucose Sensing: Evolution of Biosensor Platforms Based on Advanced Nanosystems. *Sensors* 2020 ***20***, 6013.

10. Kriechbaum, M., Heilmann, H. J., Wientjes, F. J., Hahn, M., Jany, K.-D., Gassen, H. G., Alaeddinoglu, G. (1989). Cloning and DNA sequence analysis of the glucose oxidase gene from *Aspergillus nigerNRRL-3. FEBS Letters* **255**, 63–66.

11. Lakowicz J.R. (2006) Principles of Fluorescence Spectroscopy Protein Fluorescence, 3rd edition, Springer, Boston, MA., pages 529–575.

12. Laukens, B., De Wachter, C., Callewaert, N. (2015) Engineering the *Pichia pastoris* N-Glycosylation Pathway Using the GlycoSwitch Technology. *Methods in Molecular Biology*, 103–122.

13. Leskovac, V., Trivić, S., Wohlfahrt, G., Kandrač, J., Peričin, D. (2005) Glucose oxidase from *Aspergillus niger*: the mechanism of action with molecular oxygen, quinones, and one-electron acceptors. *The International Journal of Biochemistry & Cell Biology*, **37**, 731–750.

14. Levasseur A, Drula E, Lombard V, Coutinho PM, Henrissat B (2013) Expansion of the enzymatic repertoire of the CAZy database to integrate auxiliary redox enzymes. *Biotechnol Biofuels* 6:41.

15. Levasseur, A., Lomascolo, A., Chabrol, O. *et al.* (2014) The genome of the white-rot fungus *Pycnoporus cinnabarinus*: a *basidiomycete* model with a versatile arsenal for lignocellulosic biomass breakdown. *BMC Genomics* **15,** 486.

16. LudwigLab (2018) Diaziridine-FAD: A stable cofactor for biocatalysts and a molecular probe – project summary. Visited on September 30th 2021. <https://www.ludwiglab.at/projects/project-diaziridine/>

17. Ludwig, R., Harreither, W., Tasca, F., & Gorton, L. (2010). Cellobiose Dehydrogenase: A Versatile Catalyst for Electrochemical Applications. *ChemPhysChem*, **11**, 2674–2697.

18. Ma, S., Ludwig, R. (2018) Direct electron transfer of enzymes facilitated by cytochromes. *ChemElectroChem*. **6**, 958-975

19. Navarre, W. W., & Schneewind, O. (1994) Proteolytic cleavage and cell wall anchoring at the LPXTG motif of surface proteins in Gram-positive bacteria. *Molecular Microbiology* **14**, 115–121.

20. NEB (2016) Monarch Plasmid Miniprep Kit: Instruction Manual, NEB – New England BioLabs, Ipswich. (ove NEB navode mogu ukloniti ali su spomenuti u tekstu u transformaciji plazmidda)

21. NEB (2017) NEB 5-alpha competent E. coli (High Efficiency), NEB – New England BioLabs, Ipswich.

22. Popp, M. W., Antos, J. M., Grotenbreg, G. M., Spooner, E., Ploegh, H. L. (2007) Sortagging: a versatile method for protein labeling. *Nature Chemical Biology* **3**, 707–708.

23. Posthuma-Trumpie, G. A., van den Berg, W. A. M., van de Wiel, D. F. M., Schaaper, W. M. M., Korf, J., van Berkel, W. J. H. (2007). Reconstitution of apoglucose oxidase with FAD conjugates for biosensoring of progesterone. *Biochimica et Biophysica Acta (BBA) - Proteins and Proteomics* **1774**, 803–812.

24. Potvin, G., Ahmad, A., Zhang, Z. (2012) Bioprocess engineering aspects of heterologous protein production in *Pichia pastoris*: A review. *Biochemical Engineering Journal* **64**, 91–105.

25. Rocchitta, G., Spanu, A., Babudieri, S., Latte, G., Madeddu, G., Galleri, G., Nuvoli, S., Bagella, P., Demartis, M. I., Fiore, V., Manetti, R., Serra, P. A. (2016) Enzyme Biosensors for Biomedical Applications: Strategies for Safeguarding Analytical Performances in Biological Fluids. *Sensors (Basel, Switzerland)* ***16***, 780.

26. Romero, E., Gómez Castellanos, J. R., Gadda, G., Fraaije, M. W., Mattevi, A. (2018) Same Substrate, Many Reactions: Oxygen Activation in Flavoenzymes. *Chemical Reviews* **118**, 1742–1769.

27. Sützl, L., Foley, G., Gillam, E.M.J. et al. (2019) The GMC superfamily of oxidoreductases revisited: analysis and evolution of fungal GMC oxidoreductases. *Biotechnol Biofuels* **12,** 118.

28. Sützl, L., Laurent, C.V.F.P., Abrera, A.T. et al. (2018) Multiplicity of enzymatic functions in the CAZy AA3 family. *Appl Microbiol Biotechnol* **102,** 2477–2492.

29. Turner, A. P. F. (2013) Biosensors: sense and sensibility. *Chemical Society Reviews*, **42**, 3184.

30. Vo-Dinh, T., Cullum, B. (2000) Biosensors and biochips: advances in biological and medical diagnostics. *Fresenius' journal of analytical chemistry* **366**, 540–551.

31. Westmark, U., Eriksson, K. (1974). Cellobiose:Quinone Oxidoreductase, a New Wood-degrading Enzyme from White Rot Fungi. *Acta chemical Scandinavica B* **28**, 209-214.

32. Wilson, R., Turner, A. P. F. (1992) Glucose oxidase: an ideal enzyme. *Biosensors and Bioelectronics*, **7**, 165–185.

33. Wong, C.M., Wong, K.H., Chen, X.D. (2008) Glucose oxidase: natural occurrence, function, properties and industrial applications. *Appl Microbiol Biotechnol* **78,** 927–938.

34. Zafar, M. N., Wang, X., Sygmund, C., Ludwig, R., Leech, D., Gorton, L. (2011) Electron-Transfer Studies with a New Flavin Adenine Dinucleotide Dependent Glucose Dehydrogenase and Osmium Polymers of Different Redox Potentials. *Analytical Chemistry*, **84**, 334–341.

35. Zafar, M.N., Beden, N., Leech, D. et al. (2012) Characterization of different FAD-dependent glucose dehydrogenases for possible use in glucose-based biosensors and biofuel cells. *Anal Bioanal Chem* **402**, 2069–2077.

36. Zhang, W., Li, G. (2004). Third-Generation Biosensors Based on the Direct Electron Transfer of Proteins. *Analytical Sciences*, **20**, 603–609.

STATEMENT OF ORIGINALITY

This is to certify, that the intellectual content of this thesis is the product of my own independent and original work and that all the sources used in preparing this thesis have been duly acknowledged.

_____

Name of student